Seismic stratigraphy of the Sabrina Coast shelf, East Antarctica: Early history of dynamic meltwater-rich glaciations

Aleksandr Montelli[1,†], Sean P.S. Gulick[1], Rodrigo Fernandez[1,§], Bruce C. Frederick[1,#], Amelia E. Shevenell[2], Amy Leventer[3], and Donald D. Blankenship[1]

[1]*Institute for Geophysics, Jackson School of Geosciences, University of Texas at Austin, Austin, Texas 78758, USA*
[2]*College of Marine Science, University of South Florida, Saint Petersburg, Florida 33701, USA*
[3]*Geology Department, Colgate University, Hamilton, New York 13346, USA*

ABSTRACT

High-resolution seismic data from the Sabrina Coast continental shelf, East Antarctica, elucidate the Cenozoic evolution of the East Antarctic Ice Sheet. Detailed seismic stratigraphic and facies analysis reveal the Paleogene to earliest Pliocene glacial evolution of the Aurora Basin catchment, including at least 12 glacial expansions across the shelf indicated by erosional surfaces and chaotic acoustic character of strata. Differences in facies composition and seismic architecture reveal several periods of ice-free conditions succeeded by glacial expansions across the shelf. A deep (~100 m), undulating erosional surface suggests the initial appearance of grounded ice on the shelf. Following the initial ice expansion, the region experienced an interval of open-marine to ice-distal conditions, marked by an up to 200-m-thick sequence of stratified sediments. At least three stacked erosional surfaces reveal major cross-shelf glacial expansions of regional glaciers characterized by deep (up to ~120 m) channel systems associated with extensive subglacial meltwater. The seismic character of the sediments below the latest Miocene to earliest Pliocene regional unconformity indicates intervals of glacial retreat interrupted by advances of temperate, meltwater-rich glacial ice from the Aurora Basin catchment. Our results document the Paleogene to late Miocene glacial history of this climatically sensitive region of East Antarctica and provide an important paleoenvironmental context for future scientific drilling to constrain the regional climate and timing of Cenozoic glacial variability.

INTRODUCTION

Antarctica's ice sheets were critical to the Cenozoic evolution of Earth's climate system, and they still influence global sea levels and oceanic and atmospheric circulation patterns (Kennett, 1977; Zachos et al., 2001b). Deciphering the long-term record of Antarctic ice sheet evolution on million-year to orbital time scales is essential to understanding fundamental shifts in the past global climate system, as well as future changes in ice volume and global sea levels (Golledge et al., 2015; DeConto and Pollard, 2016). Research efforts have focused on understanding the glacial history of the marine-based West Antarctic Ice Sheet (e.g., Rignot, 1998; Shipp et al., 1999; Conway et al., 1999; De Angelis and Skvarca, 2003; Larter et al., 2014). However, the dynamics of the East Antarctic Ice Sheet, the largest ice mass on Earth, have received less attention (Bart et al., 2000; Escutia et al., 2011; Mackintosh et al., 2014; Gulick et al., 2017).

Both numerical modeling and geophysical studies indicate that some parts of the East Antarctic Ice Sheet are grounded below sea level and may play a significant role in past ice dynamics and sea-level changes (Siegert et al., 2005; Rignot et al., 2008; Pritchard et al., 2009; Young et al., 2011; Passchier et al., 2011; Fretwell et al., 2012). One such region is the Aurora Basin complex (Figs. 1 and 2), which presently contains a series of subbasins characterized by a complex subglacial hydrological system, 3–5 m of sea-level equivalent ice, and outlet glaciers that are thinning and retreating (Zwally et al., 2005; Pritchard et al., 2009; Rignot et al., 2011, 2019; Greenbaum et al., 2015; Rintoul et al., 2016; Roberts et al., 2018; Mohajerani et al., 2018). Recent airborne geophysical surveys suggested that the Aurora Basin complex experienced multiple glacial variations throughout the Cenozoic (Young et al., 2011). While studies exist from onshore and on the continental slope offshore the Aurora Basin complex (e.g., Close, 2010; Young et al., 2011), little was known about past ice variations on the continental shelf until recently, when marine geophysical and geological data from the Sabrina Coast were acquired during U.S. Antarctic Program Cruise NBP14-02 (Gulick et al., 2017; Fernandez et al., 2018).

High-resolution seismic and bathymetry data collected on the Sabrina Coast shelf adjacent to the Moscow University ice shelf provide a unique opportunity to elucidate the Cenozoic glacial history of the Aurora Basin complex and examine the sedimentary architecture of the continental shelf (Gulick et al., 2017). The objectives of this study were to: (1) constrain the minimum number of glaciations since the initial ice-sheet expansion to the shelf, (2) examine the impact of glaciation on the continental shelf, and (3) investigate large-scale Paleogene to recent East Antarctic Ice Sheet dynamics in the context of global climate evolution.

DATA AND METHODS

In 2014, U.S. Antarctic Program Cruise NBP14-02 acquired 754 km of high-vertical-resolution (up to 3 m) multichannel seismic data using a 100-m-long (75 m active), 24 channel streamer and paired 45 in.^{3} (~737 cm^3) generator-injector (GI) guns. The guns were towed at a depth of 2.5–3 m and fired every 5 s, resulting in a nominal 12.5 m shot spacing. The source frequency was within the range of 20–300 Hz. The seismic data set, acquired opportunistically as ice cover and protected species within the safety zones permitted, included NW- and NE-oriented profiles that extend across the shelf (Fig. 2B). Here, we used two-way traveltime (TWT) seismic profiles for seismic stratigraphic interpretation.

†Present address: Scott Polar Research Institute, University of Cambridge, Cambridge CB2 1ER, UK; aim39@cam.ac.uk.

§Present address: Universidad Andres Bello, Departamento de Geología, Universidad de Chile, Santiago, Chile Plaza Ercilla 803, Santiago, Region Metropolitana, Chile.

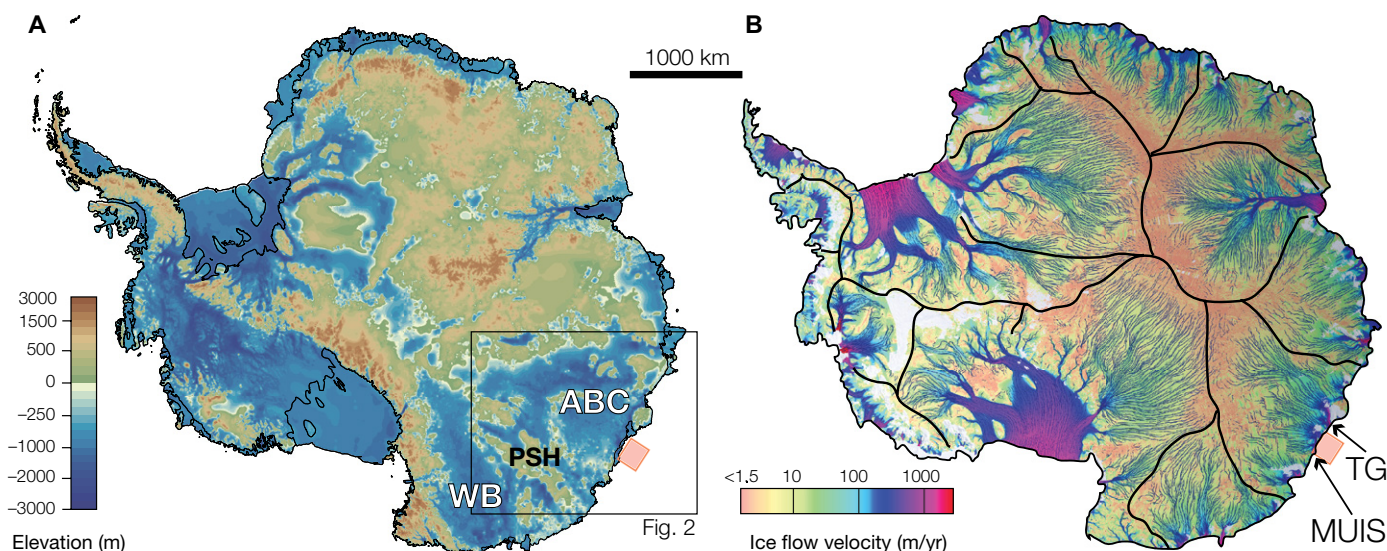#Present address: University of Kansas, Lawrence, Kansas 66045, USA.

Figure 1. (A) Bed topography of Antarctica (modified from BEDMAP2 data; Fretwell et al., 2012). Major geographic elements of Wilkes Land include: ABC—Aurora Basin complex; WB—Wilkes Basin; PSH—Porpoise Subglacial Highlands. (B) Velocity structure of Antarctica's ice drainage systems (modified from Rignot et al., 2011). Black lines mark boundaries between the major catchments. MUIS—Moscow University ice shelf; TG—Totten Glacier. In both panels, our study site is indicated by a red square.

Standard data processing included: trace regularization, bandpass and frequency-wavenumber (*f-k*) filtering, spherical divergence correction, muting, automatic gain control for display and analysis purposes, normal moveout correction, stacking, water-bottom muting, and finite-difference time domain migration. Initial results were presented in Gulick et al. (2017) and Fernandez et al. (2018). Here, we used the seismic grid to analyze seismic facies and stratigraphy in greater detail. Stratigraphic ties and facies mapping between seismic profiles were performed in Landmark's DecisionSpace Desktop application. All sediment thicknesses are presented in meters, based on a velocity within the sedimentary substrate of 2250 m/s; seafloor depths are based on a velocity in the water column of 1500 m/s. Gridded high-resolution multibeam seafloor bathymetry data complement seismic stratigraphic interpretations and were used to infer the most recent regional glacial and sedimentation history (Fernandez et al., 2018). Preliminary biostratigraphic age constraints came from marine sediment cores collected from the Sabrina Coast continental shelf (Gulick et al., 2017).

BACKGROUND

Geological Background

The rifted continental margin of Wilkes Land (~110°E–130°E) formed during the breakup Gondwana and the two-stage extension of East Antarctica and Australia. Rifting started in the Late Cretaceous through the opening of the Tasmanian Gateway in the latest Eocene (Exon et al., 2002; Lawver and Gahagan, 2003; Close, 2010; Escutia et al., 2011). The closest outcrop to the Sabrina Coast is located in the Windmill Islands, ~1000 km west of the Totten Glacier outlet (Fig. 2). Thus, major inferences about regional geology have been made using both geophysical methods and assumptions based on the distal examination of pre- and synrift sediments of the conjugate South Australian continental margin (Close et al., 2007). Further inland, series of deep subglacial basins, including the Aurora, Vincennes, and Sabrina Subglacial Basins, comprise the Aurora Basin complex (Fig. 2; Drewry, 1976; Young et al., 2011; Aitken et al., 2014, 2016). The Aurora Basin complex is separated from the Wilkes Basin by the Porpoise Subglacial Highlands (Drewry and Meldrum, 1978; Siegert et al., 2005; Donda et al., 2008), a north-south–oriented topographic high. Geophysical studies indicate that the Aurora Basin complex is bounded by regional highlands incised by deep, glacially carved valleys (Young et al., 2011). Basins within the Aurora Basin complex contain thick (up to 5 km) sedimentary infill and have generally smooth topography (Siegert et al., 2005; Young et al., 2011; Aitken et al., 2014).

Glaciological Background

Modern ice thickness and drainage pathways within the Aurora Basin complex are con-trolled by regional tectonics (Young et al., 2011; Wright et al., 2012; Aitken et al., 2014). At the lowest point of the Aurora Basin complex, the bedrock is more than 1500 m below sea level, and the ice is over 4500 m thick (Wright et al., 2012; Aitken et al., 2016). The Aurora Basin complex consists of a series of deep basins oriented nearly perpendicular to the present-day ice margin (Fig. 1). Ice discharge within the Aurora Basin complex is dominated by the fast-flowing, marine-terminating Totten Glacier and its tributaries, which currently have negative mass balances (Fig. 2A; Pritchard et al., 2009; Rignot et al., 2011; Wright et al., 2012). Beneath the ice in the Aurora Basin complex, there is a well-distributed system of subglacial channels that extend to the modern-day coastline, suggesting a potential hydrological link between regional subglacial lakes and the continental margin (Wright et al., 2012). The East Antarctic Ice Sheet is currently wet-based ice in the low-relief Aurora Basin complex sedimentary basins, whereas the rugged highlands, including the Porpoise Subglacial Highlands and portions of the Sabrina Subglacial Basin, contain cold-based ice (Siegert et al., 2005; Wright et al., 2012).

Sabrina Coast Margin Physiography and Cenozoic Sedimentation

Satellite-based bathymetry and shelf-edge data identified an irregular overdeepened shelf resulting from ice loading and glacial erosion
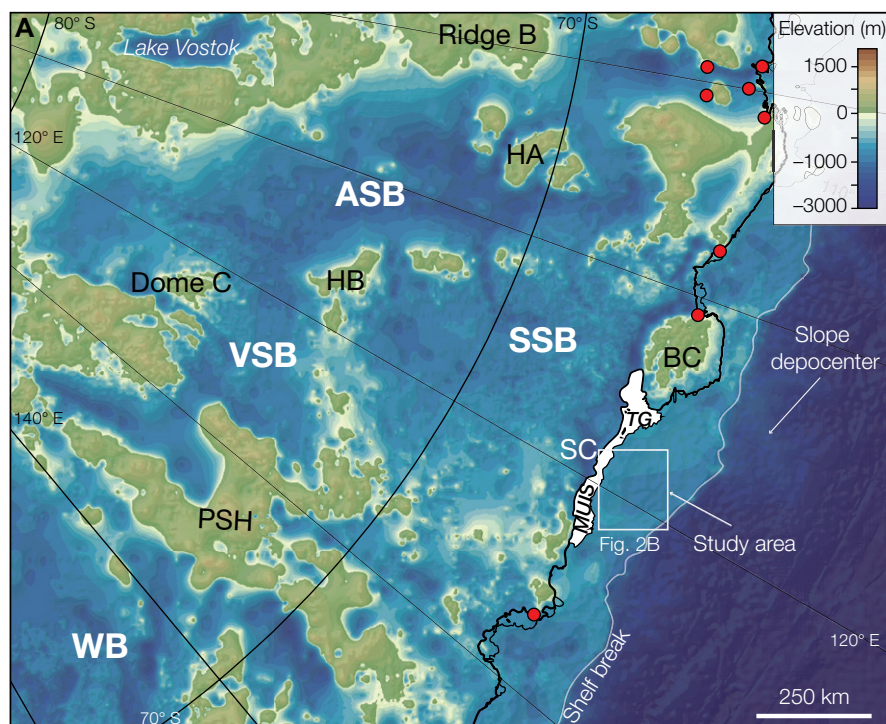
Figure 2. (A) Aurora Basin complex. Subbasins include Aurora Subglacial Basin (ASB), Sabrina Subglacial Basin (SSB), and Vincennes Subglacial Basin (VSB; after Aitken et al., 2014). Porpoise Subglacial Highlands (PSH) are to the east of Aurora Basin complex. HA—Highlands A; HB—Highlands B; SC—Sabrina Coast; MUIS—Moscow University ice shelf; TG—Totten Glacier; WB—Wilkes Basin. Study area is shown with white box. Red dots show the locations of outcrops most proximal to the study area (from Aitken et al., 2014). Map is based on BEDMAP2 data (Fretwell et al., 2012). (B) Bathymetry map showing assemblages of submarine glacial landforms present on the Sabrina Coast shelf (Fernandez et al., 2018). Thin semitransparent white lines indicate seismic profiles acquired during the NBP14-02 cruise.
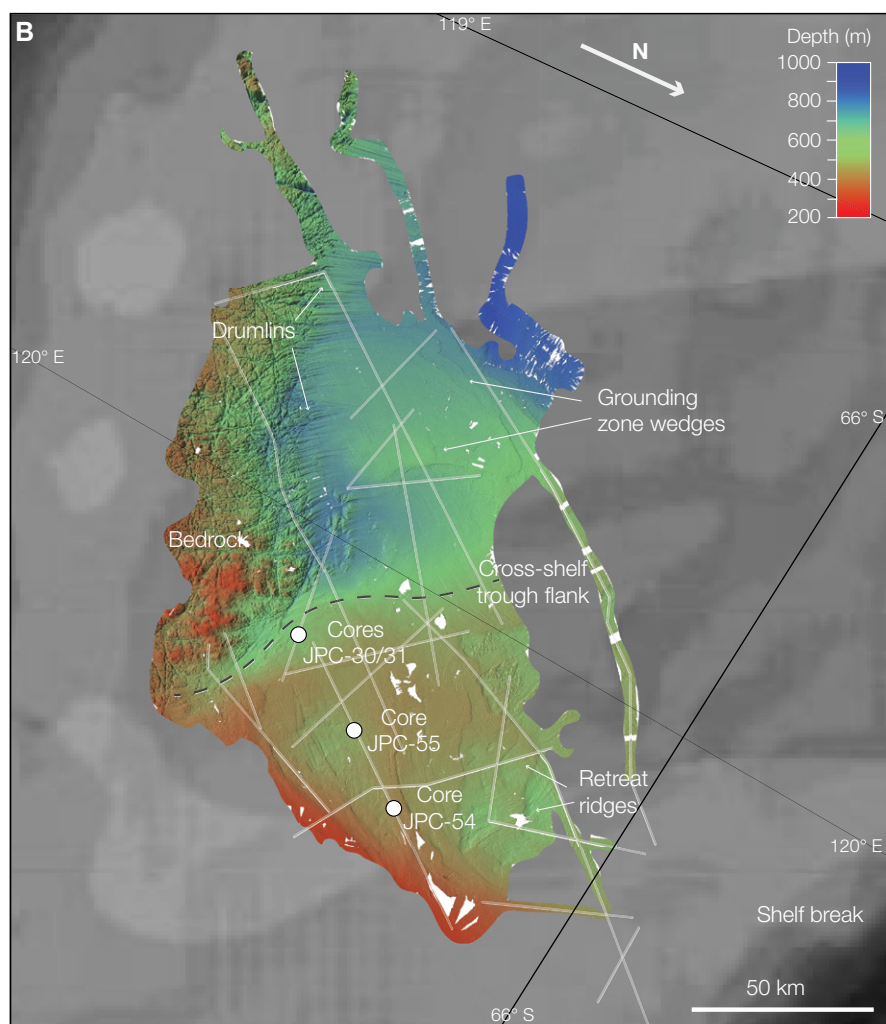
on the inner shelf (Fretwell et al., 2012). Recently, Fernandez et al. (2018) identified a network of channels incised in crystalline bedrock and partially mapped a deep basin occupied by megascale glacial lineations. This depression was proposed to be the flank of a cross-shelf trough offshore the Moscow University ice shelf (Fig. 2B). Seafloor bathymetry, derived from gravity and magnetic potential fields, reveals an interior trough that connects the subice cavity beneath Totten Glacier to the ocean, enabling warm modified Circumpolar Deep Water to enter the ice-shelf cavity and come into contact with basal ice, thereby enhancing melting (Greenbaum et al., 2015; Rintoul et al., 2016; Greene et al., 2017). The continental shelf width increases from 130 km at the eastern end of the Moscow University ice shelf terminus to 180 km at the Totten Glacier terminus (Fernandez et al., 2018), but it is only 40 km wide at the Budd Coast (Fig. 2A). A relatively gently sloping (~2°) continental slope is dominated by a few broad downslope-diverging fans and gullies (e.g., Fernandez et al., 2018), including the prominent Aurora Channel on the lower slope (~120°E; Close et al., 2007; Donda et al., 2008).

Antarctic Climate and Ice-Sheet Evolution from the Sedimentary Record

Throughout the Oligocene and early Miocene, the Antarctic ice sheet waxed and waned following astronomically paced changes in solar insolation (Naish et al., 2001; Pälike et al., 2006), preserving important glacial sedimentary archives on the shelf and slope (e.g., Anderson et al., 1980; Bart et al., 2000; Escutia et al., 2005; Gohl et al., 2013). Deep-sea oxygen isotope records suggest that ice expanded on

Antarctica ca. 34 Ma, as Earth's climate cooled, atmospheric CO_2 significantly declined, and tectonic plates reorganized (e.g., Kennett and Shackleton, 1976; Kennett, 1977; Zachos et al., 2001a; Francis et al., 2008). This period of cooling terminated with the Miocene climatic optimum, an interval of global warmth that lasted from ca. 17 to 14.5 Ma (Flower and Kennett, 1994; Shevenell et al., 2004; Warny et al., 2009; Passchier et al., 2011; Levy et al., 2016; Gasson et al., 2016; McKay et al., 2018; Sangiorgi et al., 2018). CO_2 levels dropped below 400 ppm again during the middle Miocene climate transition around 14 Ma and remained below this threshold through much of the Miocene and the Quaternary, separated by a warmer early Pliocene Epoch (ca. 5–3 Ma; Zachos et al., 2001a; Shevenell et al., 2008; McKay et al., 2009, 2016; Naish et al., 2009; Levy et al., 2016; Herbert et al., 2016).

In the Prydz Bay area of East Antarctica, middle Eocene–early Oligocene glacial conditions were recorded by Ocean Drilling Program (ODP) Leg 119 and 188 drilling data (Hambrey et al., 1991; Kuvaas and Kristoffersen, 1991; Cooper and O'Brien, 2004). Seismic data complement the drilling record, showing multiple strong mid-Miocene unconformities on the shelf produced by major glacial expansions (Cooper and O'Brien, 2004). Ice streams originated in Prydz Bay in late Miocene–early Pliocene time, complemented by seismic stratigraphic evidence from a major slope depocenter (O'Brien and Harris, 1996; O'Brien et al., 2001; Taylor et al., 2004). Chronologically constrained seismic stratigraphic studies in the Wilkes Land sector of the East Antarctic Ice Sheet have shown three major stages of ice-sheet development: (1) glacial expansion during the early Oligocene (ca. 34 and 30 Ma), followed by (2) a transition from dynamic glaciation to (3) a regime with persistent but oscillatory ice sheets, which were sensitive to warm-water incursions (Escutia et al., 2005; Sangiorgi et al., 2018). The Pliocene Epoch in Wilkes Land was marked by a major expansion of a cold-based, polar ice sheet. On the seismic stratigraphic record, these major phases of glacial expansion are recorded by two broad regional unconformities, whereas smaller-scale oscillations are suggested by numerous less pronounced erosional seismic reflectors (Escutia et al., 2005). In addition, there is seismic evidence for major, dynamic paleo–ice streams in Wilkes Land that may have shifted positions during consecutive ice-sheet expansions; however, the timing of initiation of the first ice streams in this sector of East Antarctica remains uncertain (Eittreim and Smith, 1987; Eittreim et al., 1995; Escutia et al., 2000, 2003). In the Weddell Sea sector of the East Antarctic Ice Sheet, the presence of the deep, glacially carved Thiel/Crary Trough, adjacent to the seismically imaged and chronologically constrained Crary Trough mouth fan, indicates the presence of ice streams since at least the early Miocene (Kuvaas and Kristoffersen, 1991; Hein et al., 2011).

Numerous seismic stratigraphic studies, supported by drilling data in the Ross Sea, West Antarctica, have suggested that during the late Oligocene, the early West Antarctic Ice Sheet represented multiple isolated ice caps until at least the middle Miocene, at which point they coalesced into a broad ice sheet with draining ice streams; from this point on, the West Antarctic Ice Sheet started to periodically extend to the continental shelf, as recorded by broad unconformities with trough-like geometries bounding massive seismic units (Hayes, 1975; Balshaw-Biddle, 1981; Barrett, 1986; Anderson and Bartek, 1992; Bart et al., 2000). These glacial advances became more frequent during the Pliocene–Pleistocene, and the locations of the ice streams shifted on several occasions, resulting in a complex erosional signature on strike-oriented seismic profiles (Anderson and Bartek, 1992; De Santis et al., 1997, 1999; Anderson et al., 2019). In the Amundsen Sea Embayment, where the present-day ice sheet is largely marine-based, the first evidence for glacial conditions and associated enhanced sediment flux is found within the early-middle Miocene (i.e., ca. 21–15 Ma) strata, whereas ice streams advanced across the middle shelf during the middle to late Miocene (ca. 14–9 Ma; Gohl et al., 2013; Uenzelmann-Neben and Gohl, 2014; Uenzelmann-Neben, 2018). In contrast with the Ross Sea, ice streams in Amundsen Sea were much more geographically stable since their initiation in Miocene, as inferred from similar positions of paleotroughs through the seismic stratigraphic record (Gohl et al., 2013).

In the Antarctic Peninsula, evidence for glaciation in the Neogene and Paleogene has been derived largely from sedimentary records from King George Island and James Ross Island, where alpine glaciation was initiated ca. 37–34 Ma (Smith and Anderson, 2010; Anderson et al., 2011). The Antarctic Peninsula ice sheet developed gradually, with multiple repeated advances across the continental shelf happening since the late Miocene (Smith and Anderson, 2010). Studies of the Antarctic Peninsula ice sheet off King George Island showed that outlet glaciers have repeatedly advanced across the deep Prince Gustav Channel since at least the middle Miocene (i.e., ca. 21 Ma; Camerlenghi et al., 2001; Evans et al., 2005; Nývlt et al., 2011, 2014). During the Pleistocene, the Antarctic Peninsula ice sheet was particularly dynamic, with grounded ice advancing across the continental shelf and in some areas reaching the shelf edge during at least 10 individual glacial-interglacial cycles, as revealed by multiple unconformities overlain by chaotic seismic facies and topped with coherent laminated reflections (Smith and Anderson, 2010). In terms of indirect sedimentary evidence for paleo–ice streams, the presence of the huge Belgica Trough mouth fan, comprising ~60,000 km³ of mainly glacigenic sediment on the continental slope in the Bellingshausen Sea, suggests that erosive ice streams periodically advanced to the shelf edge for at least the last 5 m.y., providing a focused source of sediment delivery (e.g., Rebesco et al., 1997, 1998, 2002; Iwai and Winter, 2002; Scheuer et al., 2006; Dowdeswell et al., 2008).

Although Antarctica's ice sheets have undergone considerable fluctuations through the Cenozoic, the early stages of ice growth and ice-sheet development remain relatively unconstrained (Kennett, 1977; Florindo and Siegert, 2009; Mudelsee et al., 2014). With regard to the East Antarctic Ice Sheet in particular, numerical models indicate that the marine-based Aurora Basin complex may be sensitive to climate fluctuations (Golledge et al., 2015, 2017; DeConto and Pollard, 2016). However, the accuracy of these models has yet to be constrained by detailed, ice-proximal records of past glaciations (e.g., Gulick et al., 2017). Here, we expand upon the results of Gulick et al. (2017) and provide a more detailed seismic stratigraphic analysis of the Sabrina Coast shelf sequences and paleoenvironmental assessment of the Aurora Basin complex, placing it in regional Antarctic context.

RESULTS: SABRINA COAST SEISMIC STRATIGRAPHY

Seismic Facies and Morphological Features

Based on the geometry and structure of internal reflections, we identified five major seismic facies that dominate the seismic sequences of the Sabrina Coast shelf. This classification is based on previous lithological and seismic investigations of high-latitude margins in both hemispheres (e.g., Carlson, 1989; Anderson and Bartek, 1992; Cai et al., 1997; Shipp et al., 1999; Bart et al., 2000; Powell and Cooper, 2002; Escutia et al., 2003; De Santis et al., 2003; Dowdeswell et al., 2007; Batchelor et al., 2013). To be consistent with the published classifications, we adopted the existing facies nomenclature (Fig. 3) from recent seismic stratigraphic studies (Shipp et al., 1999; Smith and Anderson, 2010; Batchelor et al., 2013; Zurbuchen et al., 2015; Montelli et al., 2017).
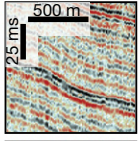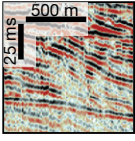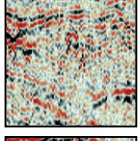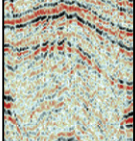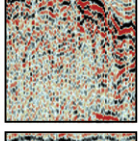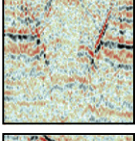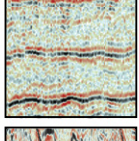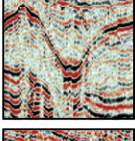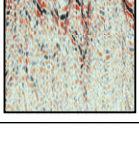
Figure 3. Seismic facies and morphological features identified within Sabrina Coast shelf seismic stratigraphic record. TWT—two-way traveltime.

(1) Facies S (Fig. 3) was identified by the well-stratified parallel to subparallel character of seismic reflectors. Reflections vary from high to low amplitude. Stratified and continuous reflections imply well-sorted sediment with consistent clast size, often deposited within a relatively low-energy depositional environment.

(2) Facies H (Fig. 3) has hummocky, irregular, channelized, mainly chaotic internal reflections, with occasional mound-shaped high-amplitude reflectors, similar to the ice-proximal facies found in the seismic stratigraphic record of the Gulf of Alaska (e.g., Powell and Cooper, 2002; Montelli et al., 2017).

(3) Facies C (Fig. 3) reflectors have an internally chaotic to poorly stratified character and form a wedge-shaped body. Facies C normally appears above truncating reflectors, suggesting erosion, poor sediment sorting, and deposition in a typically high-energy environment.

(4) Facies T (Fig. 3) was identified in sheet-like internally transparent units bounded by one or more high-amplitude parallel reflectors. This facies is similar to facies C in its internal acoustic character, but it differs in external morphology. Facies T appears above the regional erosional unconformity.

(5) Facies N (Fig. 3) is generally acoustically transparent and capped by a highly irregular, rugged high-amplitude reflection. The paucity of internal reflections and the morphology of the capping reflector are typical of acoustic basement.

We identified key morphological features based on their geometry, facies content, and relationships to bounding strata (Fig. 3). Progradational clinoforms with dipping internal reflectors of high to low amplitude occur between high-amplitude reflectors. Deep (up to ~150 ms TWT) and wide (up to 1150 m) channels truncate underlying reflectors, and the channel infills have chaotic internal character with occasional mounded, high-amplitude reflections (Fig. 3). Smaller indentations (~700 m wide and up to 40 ms TWT deep), with similar internal reflector configurations, also occur farther down section. In the upper part of the stratigraphic section, wedges with chaotic, low- to high-amplitude internal acoustic character are bounded by pronounced high-amplitude single reflectors (Fig. 4). These features are up to 100 ms TWT thick and 25 km wide.

Large-Scale Shelf Sequence Composition: Description

Seismic reflection data reveal that in the middle Sabrina Coast shelf, the acoustic basement (facies N) is shaped as an irregular surface that deepens toward the shelf break (Fig. 4). The rugged shape of the capping reflector of the mapped acoustic basement and the irregular and deeply dissected morphology of the seafloor in the inner shelf, where little or no sediment was found to overlie the basement (Fernandez et al., 2018), suggest that the acoustic basement consists of ice-sculpted bedrock (Fig. 2B). The strata overlying the acoustic basement were divided into three megasequences (MSI–MSIII; Figs. 4–7) based on major transitions between dominant seismic facies and the presence of regional erosional surfaces (Gulick et al., 2017).

Megasequence I

Megasequence I (MSI) is composed of a thick series of stratified, mostly low-amplitude, parallel reflectors of facies S that overlie the rugged surface of facies N and gently dip and thicken toward the shelf break (Figs. 4 and 5). The maximum thickness of MSI is difficult to determine due to the amplitude attenuation in the seismic record, but it reaches at least ~700 m on the modern middle shelf (Fig. 4C). Within the upper part of MSI, where seismic amplitudes are high enough to distinguish individual reflectors, there are at least 12 low-amplitude seismic units bounded by individual high-amplitude surfaces (units 1.1–1.12; Fig. 4). MSI also contains a series of progradational wedge-shaped clinoforms bounded by high-amplitude reflectors (Fig. 4). These clinoforms are found mostly within the upper part of MSI (e.g., a series of four such features is observed within units 1.7–

A

East Antarctic Ice Sheet

Moscow University Ice Shelf

66° S

N

Fig. 4B (NBP1402-07)

Fig. 4C (NBP1402-10)

x

y

x'

y'

Depth (m)
1000
800
600
400
200

Shelf break

120° E

50 km

B x Line 1402-07 x'

Channel

Trough flank

Erosional surface

−800

Facies H
2.3

MS II

2.2

Facies C

2.1

MS III 3.3

1.8

Facies S

1000

Stratified, subparallel reflectors

3.2

1.7

1.6

1.5

3.1

1.4

MS I

Acoustic basement

1.2

1.3

1200
Facies N

TWT (ms)

0 2.5 5 km

C y Line 1402-10 y'

Erosional surface

Progradational clinoforms

MS II

2.1
1.11
1.10

−800

1.9

1.8

1.7

MS III

1.6

1000 3.2

3.1

1.5

1.4

1.3 **MS I**

Acoustic basement

1.2

Downlap

1200 1.1

TWT (ms)

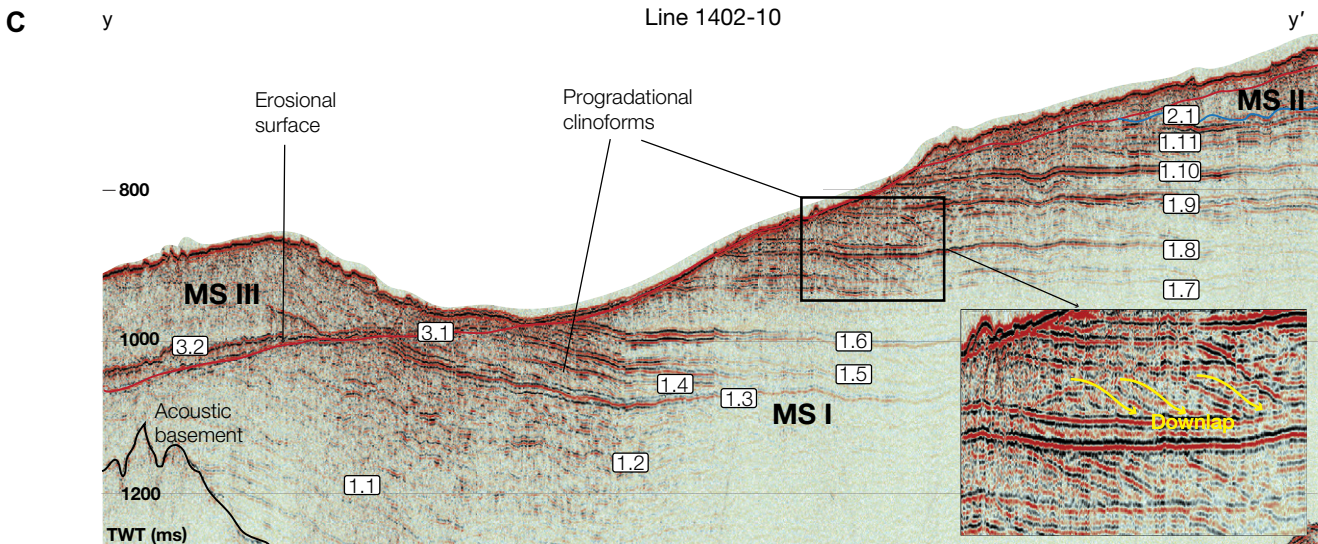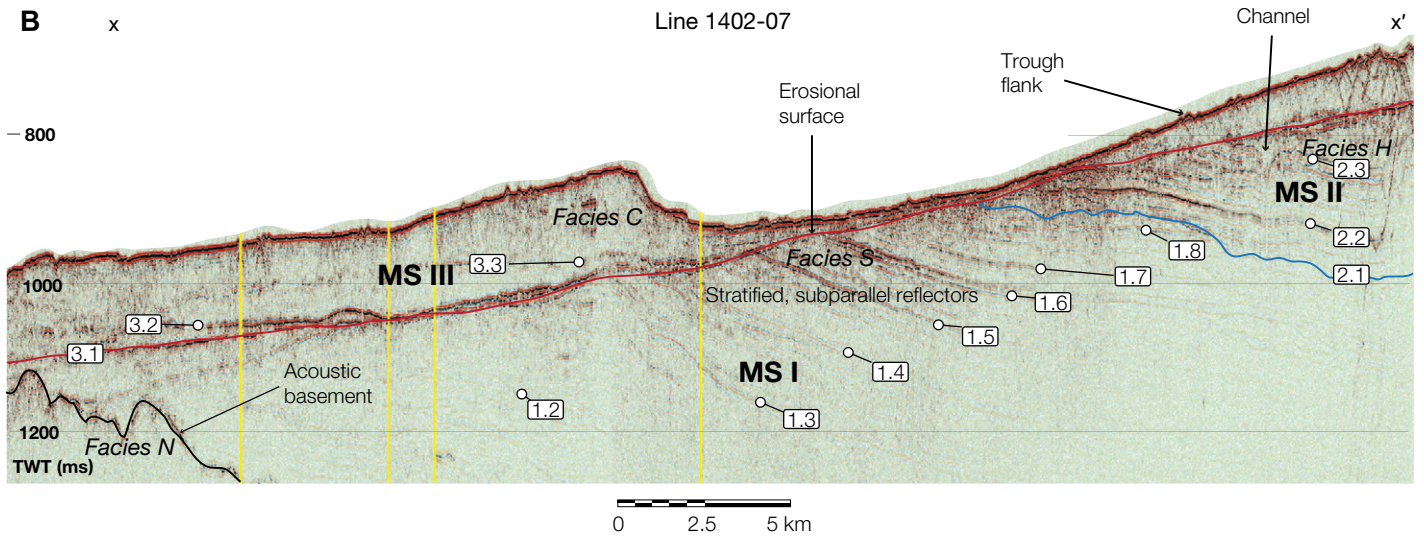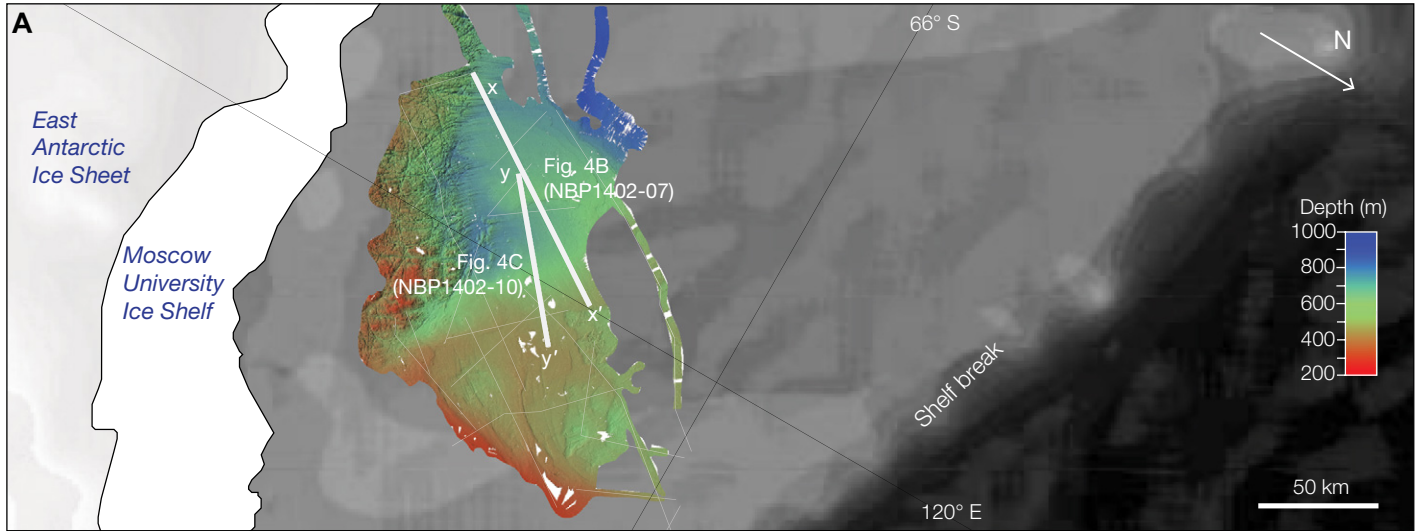Geological Society of America Bulletin

Figure 4. Seismic stratigraphy of Sabrina Coast continental shelf. (A) High-resolution multibeam seafloor bathymetry (color) collected during U.S. Antarctic Program Cruise NBP14-02 overlain on BEDMAP2 bathymetry in black and white (Fretwell et al., 2012) with interpreted seismic lines indicated (white lines). (B) Interpreted seismic profile NBP14-02-07 crossing the Sabrina Coast inner shelf. The rugged surface, highlighted in brown in lower-left corner of the seismic section, represents acoustic basement at the base of megasequence I (MSI). The undulating erosional surface 2.1 marks the base of megasequence II (MSII). The lower boundary of megasequence III (MSIII) is indicated by the regional erosional unconformity (red). Yellow vertical lines indicate where other NBP seismic lines cross. Black numbers inside white boxes are the interpreted unit boundaries within MSI (1.x), MSII (2.x), and MS III (3.x). (C) Seismic profile NBP14-02-10 crossing the Sabrina Coast inner shelf. Inset highlights the clinoforms within upper MSI. TWT—two-way traveltime.

10 [Figs. 4 and 5] and unit 1.3 [Fig. 4]). Sediment core NBP14-02 JPC-55, recovered from 15 to 20 m below the youngest clinoform, contains mica-rich silty sands of latest Paleocene age (Gulick et al., 2017). Piston core NBP1402 JPC-54, from 13 m above the youngest clinoform in MSI, contains sandy diamict of early to middle Eocene age, with centimeter-scale lonestones interpreted as ice-rafted debris (Gulick et al., 2017).

Megasequence II

Megasequence II (MSII) is up to at least ~600 m thick and is composed of several seismic units delineated by erosional surfaces and dominated by facies H, S, and C (Fig. 6). The top of MSI and the base of the MSII consist of an undulating irregularly channelized surface that truncates reflections within the upper part of MSI (Fig. 6). Gulick et al. (2017) reported 11 erosional surfaces within MSII. Here, we report an additional channelized erosional surface on the outer shelf, close to the shelf break (Fig. 7). Thus, we identified 12 major units within MSII. Each unit is distinguished by the: (1) presence of an erosional surface truncating underlying strata at its base and (2) distinctive acoustic character of internal seismic reflections. Here, the name of each unit corresponds to the name of its basal erosional surface (i.e., unit 2.1 is bounded by surfaces 2.1 at its base and 2.2 on top, and so on).

The oldest MSII units (units 2.1–2.4; e.g., those bounded by erosional surfaces 2.1–2.4, respectively) thicken landward (southwest) from ~100 m to ~200 m (Fig. 7). Erosional surfaces 2.1 and 2.4 are undulating and deeply channelized (Fig. 6). The basal surface of unit 2.1 (surface 2.1) is characterized by up to ~100 m of relief and channels up to ~7 km wide. This surface, and the strata below, dips gently (~1°) toward the shelf break. The seismic unit between surfaces 2.1 and 2.3 varies in thickness and is composed of facies H (Fig. 6). Up to ~100-m-thick layers of facies S, including a few high-amplitude reflectors, overlie the hummocky facies H (Fig. 6).

MII units 2.4 and 2.5 are composed almost entirely of facies H, with undulating basal erosional surfaces (see NBP14-02-29; Fig. 6F). The most prominent erosional surface occurs at the base of unit 2.4, with up to 120 m of vertical relief and variable morphology. Two symmetric, deeply incised channels up to 1150 m wide and ~110 m deep are observed at the eastern end of NBP14-02-29 (Fig. 6F), whereas the western end of the line consists of asymmetric channels of similar depth.

Unit 2.5 is composed of facies S, with acoustic impedance attenuation in the eastern part of the study area. This unit thins eastward from ~70 to ~10 m (Fig. 6). In the lower part of the sequence, individual reflectors onlap surface 2.5 (Fig. 6). The stratified character of unit 2.5 is interrupted by significant amplitude attenuation as the dipping unit deepens eastward. Above, erosional surface 2.6 is characterized by ~30-m-deep indentations interpreted as channels (Fig. 6H). In the plane of seismic profile NBP14-02-21, unit 2.6 is a thin package of facies C that thickens westward and is overlain by a thin drape of high-amplitude facies S. On profile NBP14-02-21, unit 2.7 is 30–150 m thick, is dominated by high-amplitude facies S, and contains small (~15 m) indentations interpreted as channels (Figs. 6F and 6H) and thin layers of acoustically transparent facies C. A layer of facies S present in the upper part of unit 2.8 pinches out eastward and is separated from neighboring units by high-amplitude draping reflections.

Surface 2.9 truncates unit 2.8, is dominated by up to ~40 m indentations (Fig. 7), and defines the base of the relatively thin (~50 m) unit 2.9, composed of facies C. The undulating erosional surface 2.9 is morphologically similar to surface 2.8, with slightly deeper incisions. Up section, unit 2.10 consists of ~50 m of facies C overlain by draping layers of low-amplitude facies S and a series of thin high-amplitude reflections similar to those observed within unit 2.8 on seismic profile NBP14-02-29. Surface 2.11 truncates the reflectors of unit 2.10 and contains small

(~10 m) indentations. Unit 2.11, identified from seismic profiles NBP14-02-21 and NBP14-02-28 (Fig. 6), consists of two intervals of facies C separated by thin high-amplitude draping reflectors. The most distal seismic profile, NBP14-02-33a (Fig. 7), shows evidence for erosional surface 2.12 with two channels incised up to 50 m deep. Further up section, the examination of younger MSII is precluded by the lack of seismic data coverage on the outer shelf and the upper slope (Fig. 2B).

Megasequence III

Megasequence III (MSIII) is composed of irregular stacked wedges of chaotic facies C and sheetlike facies T above the prominent regional erosional unconformity (3.1), which truncates dipping strata within MSII (Fernandez et al., 2018). At least two ubiquitous erosional surfaces (3.2 and 3.3) are preserved within MSIII (Figs. 6 and 7). The thickness of MSIII is laterally variable (0–200 m) on the Sabrina Coast shelf and is generally smaller toward the northeast. Diatom biostratigraphy indicates that the youngest age of the regional unconformity is late Miocene (ca. 7–5.5 Ma; Gulick et al., 2017). No channels were observed within MSIII.

DISCUSSION

Sabrina Coast Paleoenvironmental Evolution

Megasequence I: Fluvial/Glaciofluvial Sedimentation

Due to the lack of stratigraphic evidence for diagnostic glacial features and sediments within the older part of MSI (Gulick et al., 2017), we infer that the sediments comprising MSI were deposited in a preglacial environment. The alternating parallel and prograding strata (clinoforms) in the seismic stratigraphic record within MSI are interpreted as regression-transgression sequences in response to fluctuations in sea level and sediment supply. The series of clinoforms are thus interpreted as deltas of fluvial and/or glaciofluvial origin (Fig. 5). Within the youngest part of MSI, the presence of ice-rafted debris suggests the arrival of marine-terminating glaciers at the Sabrina Coast by the middle Eocene (Gulick et al., 2017). However, the lack of glacial erosional features on the continental shelf, such as truncation and incision of MSI strata, implies that regional glaciers did not extend farther than the innermost continental shelf.

Megasequence II: Polythermal Glacial Sedimentation

The high relief (more than 100 m) of the undulating erosional surfaces within the older
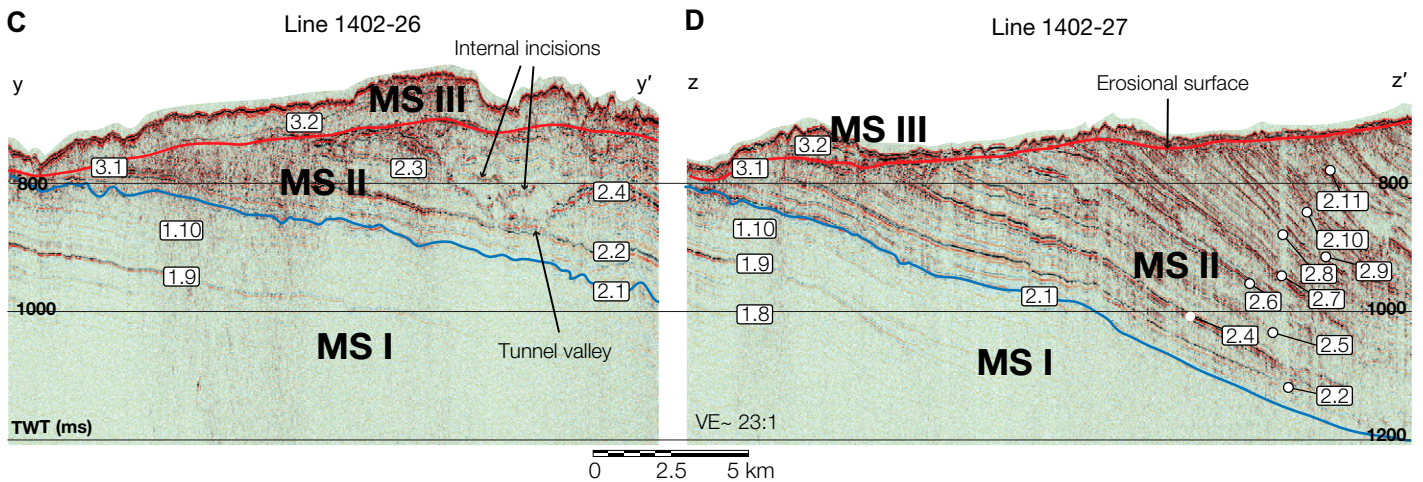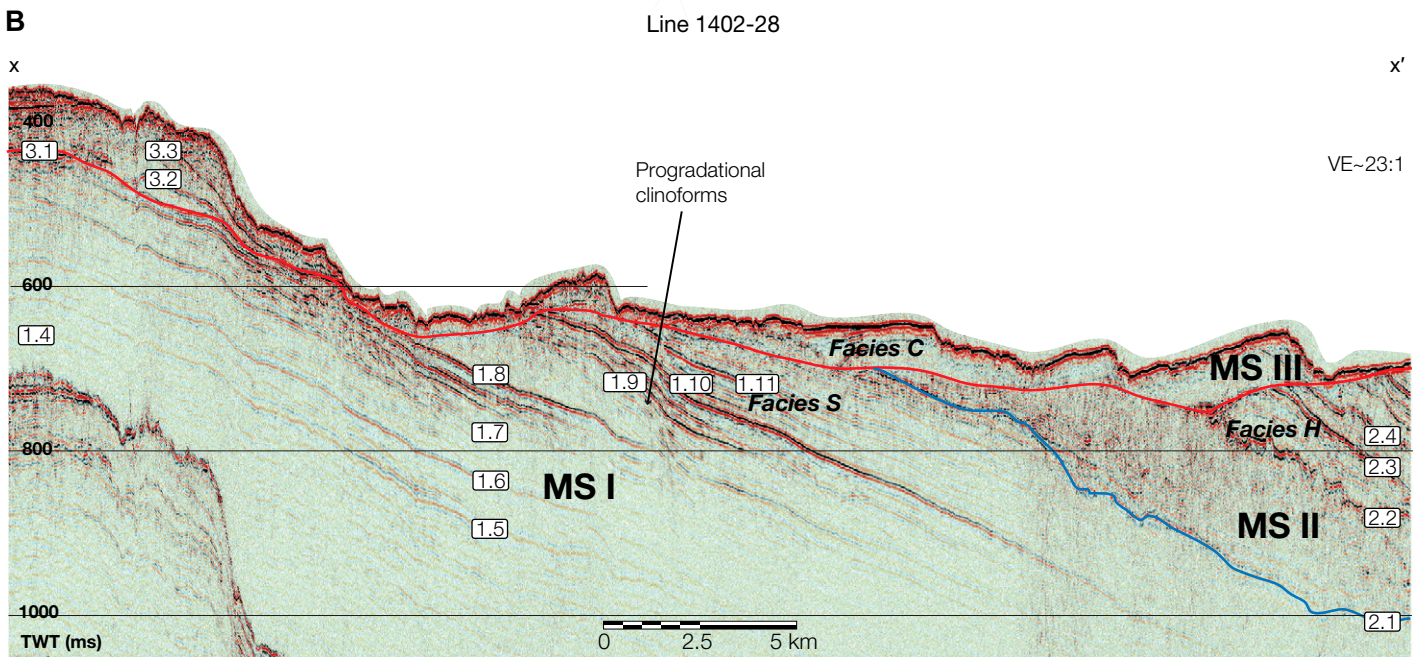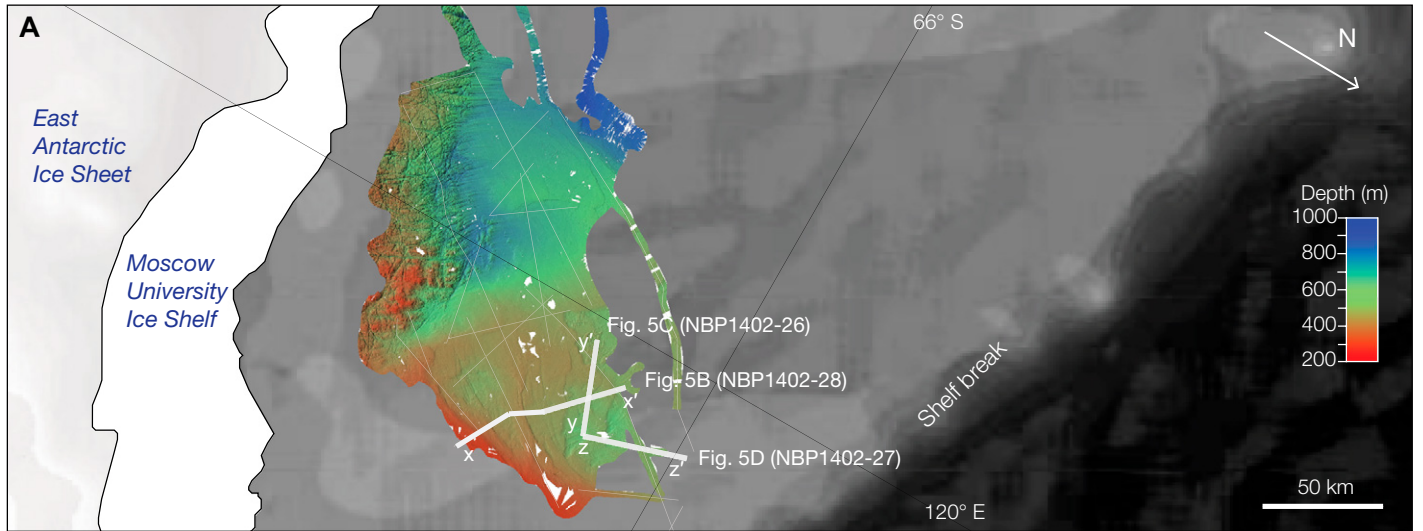
Figure 5. Seismic stratigraphy of the Sabrina Coast continental shelf. (A) High-resolution sea-floor bathymetry of the study area collected by U.S. Antarctic Program Cruise NBP14-02 (color) and BEDMAP2 bathymetry (black and white; Fretwell et al., 2012) with interpreted seismic lines (white lines). (B) Along-dip seismic profile, NBP14-02-28, across the middle Sabrina Coast shelf. (C) Along-strike seismic profile, NBP14-02-26, across the middle Sabrina Coast shelf. Cross section of a deep erosional feature, interpreted as tunnel valley (Gulick et al., 2017), is indicated within the lower section of megasequence II (MSII). (D) Along-dip seismic profile, NBP14-02-27, across the outer Sabrina Coast shelf. Black numbers inside white boxes are the interpreted unit boundaries within MSI (1.x), MSII (2.x), and MS III (3.x). TWT—two-way traveltime; MSI— megasequence I; MSIII—megasequence III; VE—vertical exaggeration.

←——————

units of MSII (e.g., surfaces 2.1 and 2.4) suggests that these features were not likely formed by fluvial incision during lowstands (Huuse and Lykke-Andersen, 2000; van der Vegt et al., 2012). This interpretation is supported by previous studies showing that Eocene and Oligocene eustatic sea-level fluctuations likely did not exceed ~50 m (Miller et al., 2005; Kominz et al., 2008), and the East Antarctic continental shelf continued to undergo tectonic subsidence until the Miocene (Escutia et al., 2011). We note that isostatic flexural uplift could have played a role if ice was building up farther inland. However, evidence for a glacial interpretation of their origin includes the observed undulating thalwegs of the erosional surfaces and anastomosing pattern of channel systems within younger surfaces (e.g., surface 2.4) and the lack of infill facies such as foreset geometries compatible with fluvial lateral accretion, or levees, or facies compatible with floodplain deposits. Henceforth, we interpret the mapped erosional features of MSII as having formed at the base of the ice sheet, close to the terminus, during intervals of significant subglacial meltwater flux from the ice-sheet interior to the margin (e.g., Ó Cofaigh, 1996; Huuse and Lykke-Andersen, 2000; Lowe and Anderson, 2002; Denton and Sugden, 2005; Domack et al., 2006; Lonergan et al., 2006; Kristensen et al., 2008; Smith et al., 2009; Stewart et al., 2012; Dowdeswell et al., 2016).

Overlying undulating erosional surface 2.1, there is a thick cover of stratified facies S, which suggests an interval of ice-proximal open-marine conditions on the shelf. Variations in acoustic impedance within the facies are related to changes in grain size and/or clast content and may reflect glacial and/or shoreline proximity (e.g., Cai et al., 1997; Naish et al., 2001; Batchelor et al., 2013; Dowdeswell et al., 2014). Thus, the low-amplitude, almost-transparent facies S may reflect a single depositional environment with no significant lithologic changes. However, recent drilling of similar stratified sequences in the Ross Sea recovered massive to stratified diamictites with variable clast content (McKay et al., 2018). Thus, while facies S may be indicative of an open-marine setting, the exact degree

of ice proximity cannot be derived from seismic data alone. High-amplitude reflectors with traces of shallow channelization within facies S might represent short intervals of ice advance, with subsequent development of shallow proglacial fluvial complexes. However, additional evidence for ice advance is not found until the appearance of another series of deeply incised channels in unit 2.2 (Fig. 6).

The absence of facies S within unit 2.4 argues against an ice-distal depositional environment due to significant glacial retreat. Rather, the ice-sheet front would have oscillated across the shelf without retreating farther inland, leading to the absence of interbedded, stratified sediment. Unit 2.4 consists of facies H and is bounded by channelized surfaces, which likely reflect the progradation of the glacial and proglacial environments onto the shelf, with abundant meltwater required to produce significant channelization and sediment transport (Fig. 5). The overall northward thinning of units 2.1–2.4 may reflect: (1) deeper erosion of unit 2.1 to the north and/or (2) enhanced deposition of units 2.1 and 2.2 in the south. Incised stratified and semitransparent reflectors within units 2.5–2.12 (Figs. 6 and 7) suggest repeated cycles of ice advance followed by retreat and subsequent open-marine sedimentation. The seismic character of units 2.5–2.8 suggests an interval of open-marine conditions interrupted by several meltwater-rich glaciations. Units 2.9–2.11 suggest a similar depositional environment, but with greater volumes of subglacial meltwater than in units 2.5–2.8. Unit 2.12 documents ice close to the inner shelf, but no conclusive evidence exists for grounded ice on the shelf.

Overall, Sabrina Coast continental shelf seismic data suggest a dynamic regional glacial evolution in the late Paleogene and early Neogene (Fig. 8), including ice advance across the inner and middle shelf on at least 12 occasions (erosional surfaces 2.1–2.12). Differences in facies composition and sequence architecture in MSII suggest glacial fluctuations of considerable magnitude, from extensive polythermal glaciers covering significant parts of the shelf to open-marine, ice-distal environments. In other

Antarctic continental margins, a similar, overall oscillatory character of Oligocene to mid-Miocene glacial dynamics has been observed from seismic stratigraphy in Wilkes Land, where initial glacial expansion was followed by several phases of polythermal glacial advance and retreat, which resulted in deposition of low-angle prograding foresets bounded by smaller-scale erosional unconformities (Escutia et al., 2005). Similarly, alternating seismically transparent grounding zone deposits overlain by packages of stratified sediment also dominate the Oligocene–Miocene shelf stratigraphy in the Ross Sea (e.g., Brancolini et al., 1995; McKay et al., 2018). However, in contrast with other Antarctic continental shelves, Sabrina Coast seismic stratigraphy uniquely demonstrates multiple generations of deep meltwater channels that have not been observed anywhere else in Antarctica. These features are particularly deep in the oldest glacial sedimentary section (Figs. 5, 6, and 8), suggesting extensive, abundant meltwater systems during the initial glacial expansion (discussed in more detail in subsequent section on "Sabrina Coast Tunnel Valley System").

A complete depositional history of MSII is not possible to infer due to the prominent regional erosional event (surface 3.1) that truncates MSII strata and marks a major ice-sheet expansion in the late Miocene, likely in association with global cooling (Herbert et al., 2016; Kingslake et al., 2018). We suggest that during deposition of MSII, the Aurora Basin complex was drained by series of highly dynamic, meltwater-rich outlet glaciers. There is no seismic evidence for large fast-flowing ice streams or overdeepening related to large ice-sheet expansion during MSII strata deposition, although we cannot exclude that it may be potentially preserved in the paleo–outer shelf and slope section, which is located beyond the coverage of seismic data used in this paper.

Megasequence III: Glacial Sedimentation Following Major Ice-Sheet Expansion

The first evidence for major ice-sheet expansion and associated overdeepening coincides with the regional erosional surface 3.1, which truncates both MSII and MSIII strata. In terms of broad-scale Cenozoic paleoenvironmental change, three major phases of deposition observed in the Sabrina Coast (i.e., preglacial, oscillatory ice-sheet growth and decay, and major ice-sheet dominated) have been also reported from seismic architecture of several other continental shelves in Antarctica, although the timing of these phases is regionally variable (e.g., Eittreim et al., 1995; ten Brink and Schneider, 1995; De Santis et al., 1999; Bart et al., 2000; Anderson and Shipp, 2001; Bart et al., 2003;
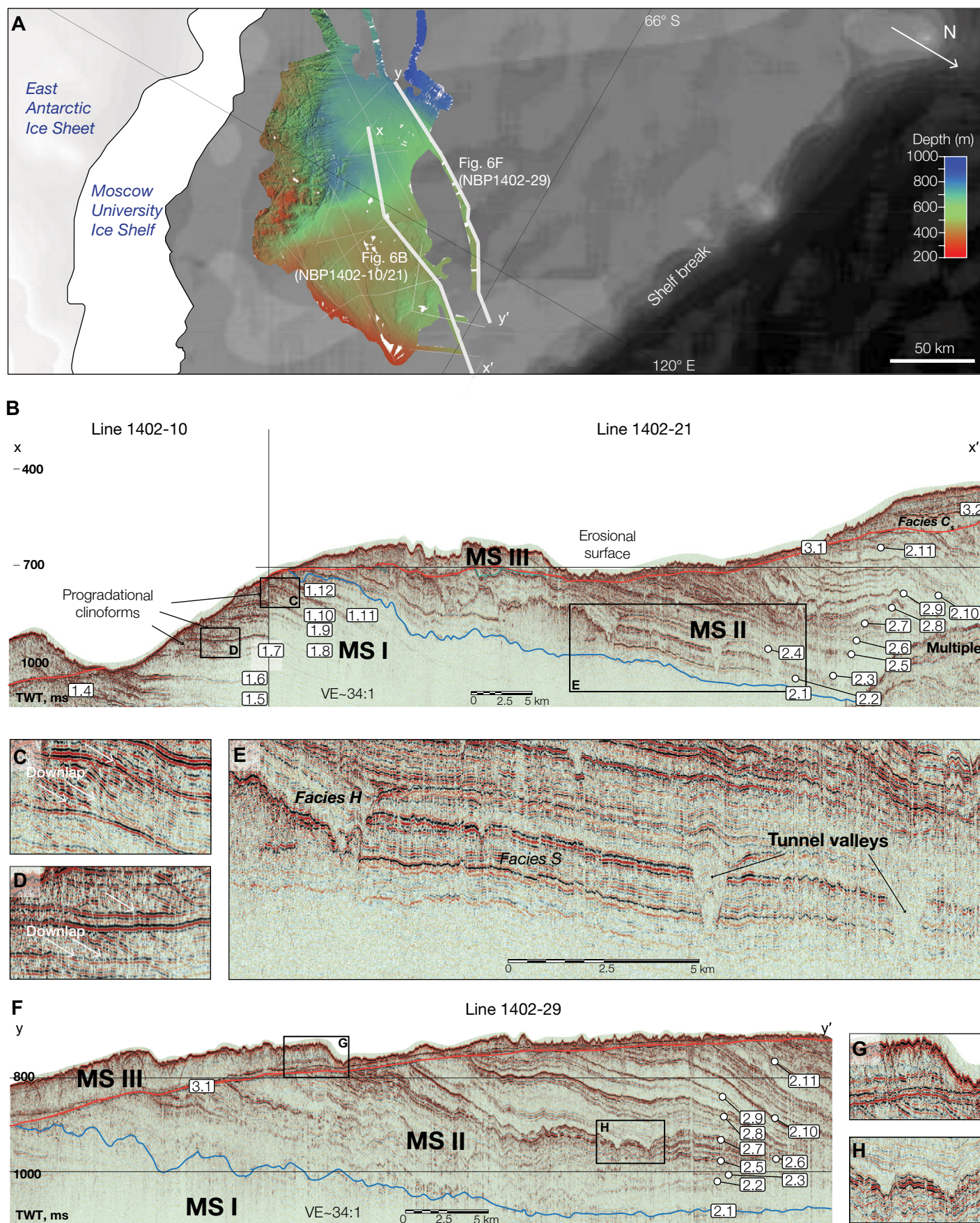
Figure 6. Seismic stratigraphy of Sabrina Coast continental shelf. (A) High-resolution sea-floor bathymetry of the study area from NBP14-02 (Fernandez et al., 2018) and BEDMAP2 bathymetry (black and white; Fretwell et al., 2012) with interpreted NBP14-02 seismic lines (white lines). (B) Merged along-strike seismic profiles NBP14-02-10 and NBP14-02-21, crossing the inner to midshelf. (C–D) Expanded views of progradational clinoforms found within the upper section of megasequence I (MSI). (E) Expanded view of channels incised into lower megasequence II (MSII) strata. (F) Along-strike seismic profile NBP14-02-29, crossing the Sabrina Coast shelf. (G) Expanded view of an acoustically chaotic wedge-shaped feature, interpreted as grounding-zone wedges within megasequence III (MSIII; Fernandez et al., 2018). (H) Expanded view of channels found in the middle section of MSII. Black numbers inside white boxes are the interpreted unit boundaries within MSI (1.x), MSII (2.x), and MS III (3.x). TWT—two-way traveltime; VE—vertical exaggeration.

De Angelis and Skvarca, 2003; Cooper and O'Brien, 2004; Escutia et al., 2005; Smith and Anderson, 2010; Bart and Iwai, 2012; McKay et al., 2018). Seismic data presented here indicate that regional overdeepening probably occurred in the late Miocene, following an interval of shelf progradation in association with ice-sheet expansion (Gulick et al., 2017).

The regional ice expansion indicated by erosional surfaces 3.1, 3.2, and 3.3 likely reflects the Pliocene–Pleistocene advance and retreat of a large polar East Antarctic Ice Sheet. The small number of erosional seismic surfaces suggests a much less dynamic ice sheet, compared to, for example, the Antarctic Peninsula region, where the West Antarctic Ice Sheet advanced and retreated at least 10 times over the Pleistocene, as revealed by stacked, massive, chaotic seismic facies bounded by erosional unconformities (Smith and Anderson, 2010). Furthermore, previous studies of the West Antarctic Ice Sheet in the Ross Sea found sedimentary evidence for ice-sheet collapse and associated open-marine conditions that prevailed during the early Pliocene (5–3 Ma), possibly due to the higher sensitivity and retreat of the largely marine-based West Antarctic Ice Sheet (Naish et al., 2009). However, despite the Aurora Basin being part of the marine-based sector of the East Antarctic Ice Sheet, evidence for similar ice-sheet disintegration during the early Pliocene in Sabrina Coast, such as stratified reflectors overlying glacial facies, is not found in our data, highlighting important regional differences in the Antarctic ice-sheet evolution. A more detailed analysis of MSIII can be found in Fernandez et al. (2018).

Sabrina Coast Tunnel Valley System

Tunnel valleys were observed in five erosional surfaces (e.g., 2.3–5, 2.8, and 2.9), suggesting at least five meltwater-rich glaciations (Gulick et al., 2017). A particularly striking example of tunnel valleys is found within undulating erosional surface 2.4, where two symmetric channels incised into underlying strata (Fig. 6).

They are ~1150 m wide and ~120 m deep, with flank gradients ranging between 12° and 15° (Fig. 6). The asymmetric configuration of channels to the west of these tunnel valleys (Fig. 6) suggests that the channel system was complex and anastomosing, which is common globally within subglacial meltwater systems (e.g., Denton and Sugden, 2005; Lonergan et al., 2006; Smith et al., 2009; Bjarnadóttir et al., 2017).

We compared the morphology of the tunnel valley cross-section profiles with similar features in the North Sea, Barents Sea, and Gulf of Alaska (Fig. 9), where these features have been previously observed (Lonergan et al., 2006; Kristensen et al., 2008; Berger et al., 2008; Stewart et al., 2012; Bjarnadóttir et al., 2017). Morphometrically, these channels are similar to subglacial tunnel valleys documented in the Northern Hemisphere (Fig. 9; e.g., Ó Cofaigh, 1996; Huuse and Lykke-Andersen, 2000; Lowe and Anderson, 2003; Denton and Sugden, 2005; Lonergan et al., 2006; Kristensen et al., 2008; Stewart et al., 2012), but they are up to four times smaller than the largest examples of tunnel valleys, which were mapped and reported from the North Sea (Praeg, 2003).

Extensive subglacial meltwater channel systems incised into crystalline bedrock have been reported from the inner-shelf sections of cross-shelf troughs in West Antarctica (Anderson and Shipp, 2001; Lowe and Anderson, 2002; Ó Cofaigh et al., 2002; Domack et al., 2006; Anderson and Fretwell, 2008; Graham et al., 2009; Nitsche et al., 2013; Livingstone et al., 2012). However, only limited evidence exists from the Ross Sea and Dry Valleys for tunnel valleys carved into sediments (e.g., Sugden et al., 1995; Denton and Sugden, 2005; Wellner et al., 2006; Lewis et al., 2006, 2008). In contrast, tunnel valleys shown here are the first deep, buried sedimentary meltwater features conclusively reported from the Antarctic continental margin. Both the composition of the glacial substrate and the presence of subglacial meltwater influence glacier and ice-sheet stability (e.g., Blankenship et al., 1986; Alley et

al., 1987; Lowe and Anderson, 2003; Wingham et al., 2006; Siegert et al., 2007; Golledge et al., 2012; Simkins et al., 2017). The seismic data presented here document the first conclusive evidence of a buried, deep, extensive and complex sedimentary tunnel valley system in East Antarctica, with important implications for Paleogene to Neogene East Antarctic Ice Sheet subglacial meltwater regime and numerical modeling experiments that aim to simulate the subglacial conditions during early stages of ice-sheet growth.

Numerical modeling of meltwater dynamics in an overpressured subglacial system suggests that tunnel valleys are produced when meltwater exceeds the capacity of drainage through permeable subglacial till (Piotrowski, 1997). These conditions can occur during (1) spontaneous, catastrophic outburst events, such as collapse of ice-dammed lakes and meltwater floods (Wingfield, 1990; Shaw, 2002), or from (2) episodic, repeated erosion produced in a more gradual fashion by a subglacial meltwater drainage system (Lonergan et al., 2006; Livingstone and Clark, 2016). Possible explanations for the substantial difference in magnitude of incision observed in East Antarctica and the North Sea thus may be related to a number of factors, including the number and duration of meltwater discharge events; type of subglacial substrate; ice-sheet thickness; shelf depth at the base of grounded ice and the distance from the ice-sheet margin at which the meltwater drainage system was initiated.

Additional explanations for high-amplitude early glacial erosion arise from paleoenvironmental considerations. By the early Eocene, the opening of the Tasmanian Gateway had already begun, allowing for the development of shallow marginal seas (Exon et al., 2002; Stickley et al., 2004). Considering that both regions surrounding the Aurora Basin complex (i.e., Wilkes Land and Gamburtsev Mountains) were at higher elevation compared to the current bed topography (e.g., Stocchi et al., 2013), such a paleogeographic setting may have favored the development of temperate climates with winter snow (Francis, 1999, 2000). As climate cooled down by the late Eocene–early Oligocene, it might have allowed more snow to accumulate and develop very dynamic, erosive, alpine and tidewater glacial systems similar to those currently observed in the Gulf of Alaska (Fig. 9). Such a paleoenvironmental setting could provide additional explanation for the deep, meltwater-related glacial erosion features observed on the Sabrina Coast and their similarity to early glacial strata features of the Gulf of Alaska (e.g., Berger et al., 2008; Elmore et al., 2013; Montelli et al., 2017).
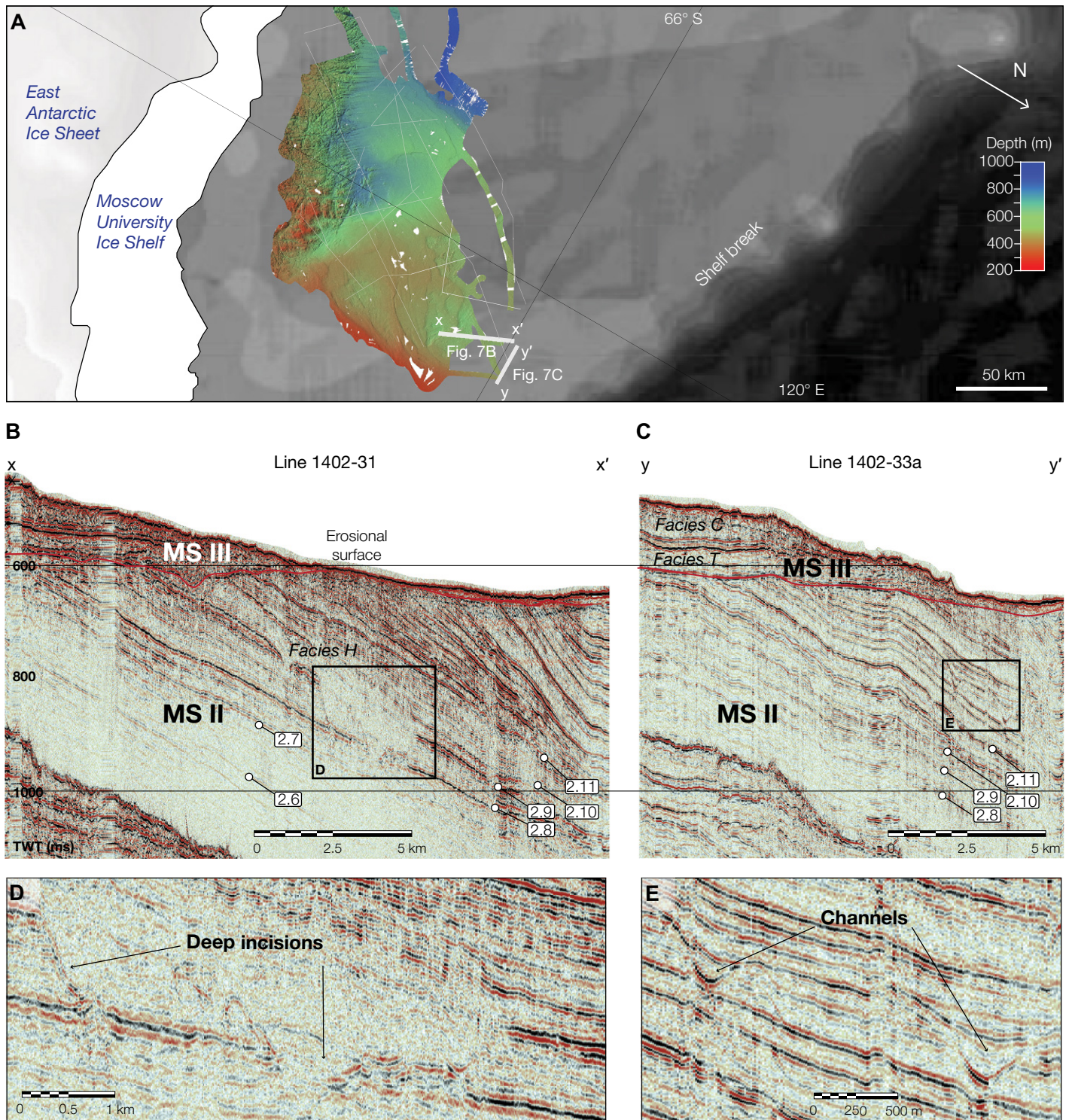
Figure 7. Seismic stratigraphy of the Sabrina Coast continental shelf. (A) High-resolution seafloor bathymetry of the study area (color) and BEDMAP2 bathymetry (black and white; Fretwell et al., 2012) with interpreted seismic lines (white lines). (B) Seismic profiles NBP14-02-31 from the outer shelf. (C) Seismic profile NBP14-02-33a across the outer Sabrina Coast shelf. (D) Expanded view of deep incisions within the older units of megasequence II (MSII). (E) Expanded view of channels found in the upper section of MSII. Black numbers inside white boxes are the interpreted unit boundaries within MSI (1.x), MSII (2.x), and MS III (3.x). MSIII—megasequence III; TWT—two-way traveltime.
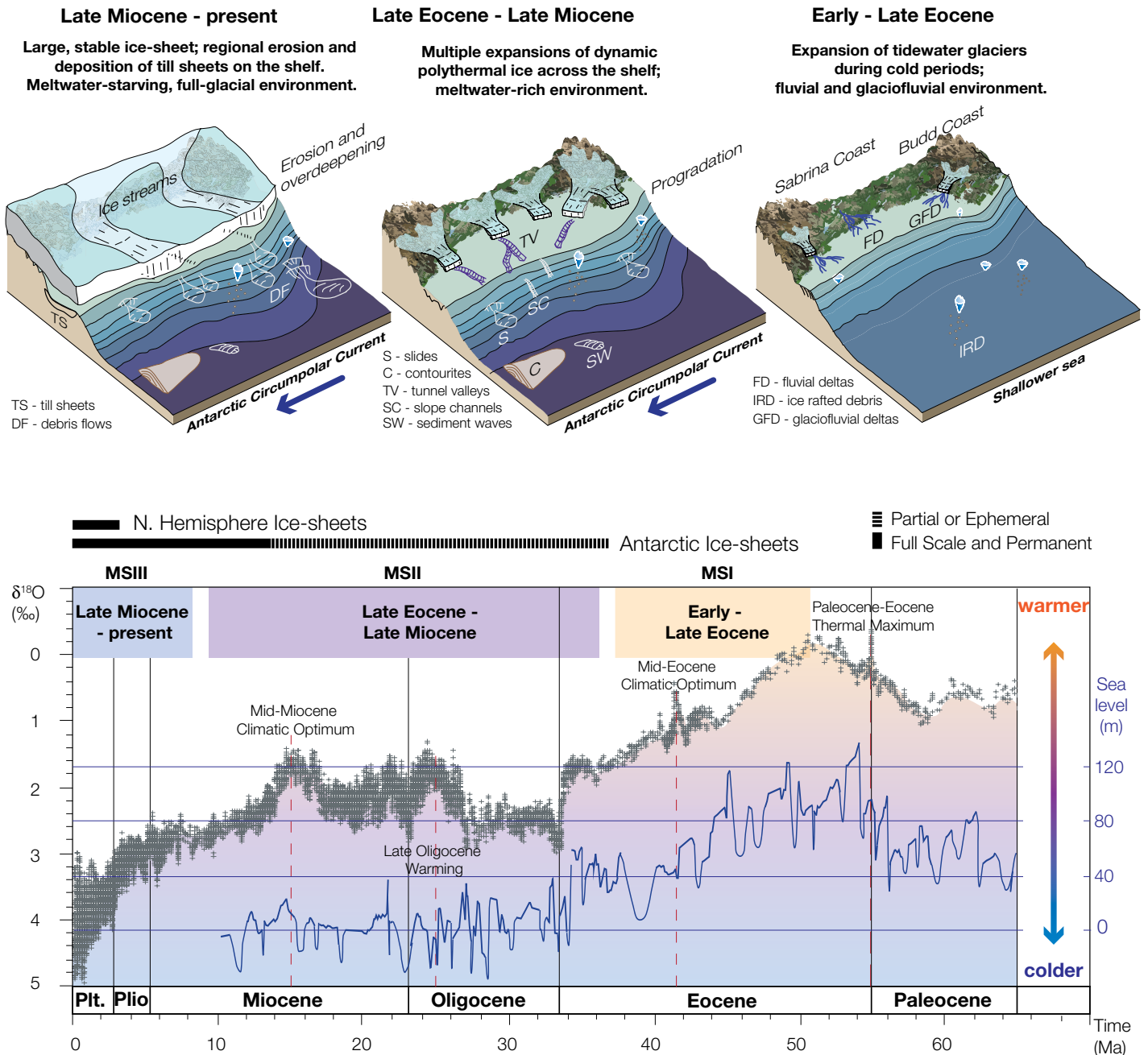
Figure 8. Proposed possible timing of major glacial expansions along Sabrina Coast in Oligocene–middle Miocene juxtaposed with global oxygen isotope curve by Zachos et al. (2001b) and global sea-level curve by Kominz et al. (2008). Plio—Pliocene; Plt—Pleistocene; MSI—megasequence I; MSII—megasequence II; MSIII—megasequence III.

CONCLUSIONS

The first high-resolution seismic data from the Sabrina Coast continental shelf reveal the pre–late Miocene evolution of the large Aurora Basin complex and its transition from fluvial and glaciofluvial sedimentary environment through a prolonged interval of multiple meltwater-rich polythermal glaciations. During this pre–late Miocene period of polythermal glaciation, seismic stratigraphy indicates periods of retreating glacial conditions interrupted by expansions of temperate meltwater-rich glacial ice from the Aurora Basin complex catchment. We interpret at least 12 glacial expansions across the shelf, as indicated by erosional surfaces and the chaotic acoustic character of strata. We report finding the first conclusive evidence of a deep, extensive tunnel valley system incised into sedimentary substrate from an Antarctic continental margin from early polythermal glaciations. Discharge of huge volumes of subglacial meltwater associated with the formation of these extensive incision systems may have contributed to changes in regional and/or global climate. Our results provide paleoenvironmental context for future studies of the Cenozoic climatic evolution in East Antarctica and an important proxy for ice-sheet dynamics under slightly warmer-than-present (i.e., over 400 ppm CO_2 levels) climate conditions. Dipping shelf
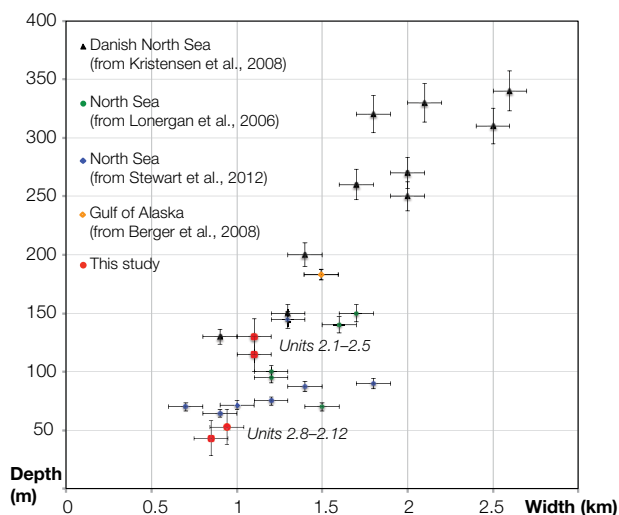
strata and distinct well-preserved morphological features make this region a perfect target for future scientific drilling investigations designed to further elucidate the early behavior of the East Antarctic Ice Sheet and provide critical baseline constraints for future global climate models.

REFERENCES CITED

Aitken, A., Young, D., Ferraccioli, F., Betts, P., Greenbaum, J., Richter, T., Roberts, J., Blankenship, D., and Siegert, M., 2014, The subglacial geology of Wilkes Land, East Antarctica: Geophysical Research Letters, v. 41, no. 7, p. 2390–2400, https://doi.org/10.1002/2014GL059405.
Aitken, A., Roberts, J., Van Ommen, T., Young, D., Golledge, N., Greenbaum, J., Blankenship, D., and Siegert, M., 2016, Repeated large-scale retreat and advance of Totten Glacier indicated by inland bed erosion: Nature, v. 533, no. 7603, p. 385, https://doi.org/10.1038/nature17447.
Alley, R.B., Blankenship, D., Bentley, C.R., and Rooney, S., 1987, Till beneath ice stream B: 3. Till deformation: Evidence and implications: Journal of Geophysical Research–Solid Earth, v. 92, no. B9, p. 8921–8929, https://doi.org/10.1029/JB092iB09p08921.
Anderson, J.B., and Bartek, L.R., 1992, Cenozoic glacial history of the Ross Sea revealed by intermediate resolution seismic reflection data combined with drill site information, in Kennett, J.P., and Warkne, D.A., eds., The Antarctic Paleoenvironment: A Perspective on Global Change: Part One: American Geophysical Union Antarctic Research Series 56, p. 231–264.
Anderson, J.B., and Fretwell, L.O., 2008, Geomorphology of the onset area of a paleo–ice stream, Marguerite Bay, Antarctic Peninsula: Earth Surface Processes and Landforms, v. 33, no. 4, p. 503–512.
Anderson, J.B., and Shipp, S.S., 2001, Evolution of the West Antarctic Ice Sheet, in Alley, R.B., and Bindschadler, R.A., eds., The West Antarctic Ice Sheet: Behavior and

Environment: American Geophysical Union Antarctic Research Series 77, p. 45–57, https://doi.org/10.1029/AR077p0045.
Anderson, J.B., Kurtz, D., Domack, E., and Balshaw, K., 1980, Glacial and glacial marine sediments of the Antarctic continental shelf: The Journal of Geology, v. 88, no. 4, p. 399–414, https://doi.org/10.1086/628524.
Anderson, J.B., Warny, S., Askin, R.A., Wellner, J.S., Bohaty, S.M., Kirshner, A.E., Livsey, D.N., Simms, A.R., Smith, T.R., Ehrmann, W., Lawver, L.A., Barbeau, D., Wise, S.W., Kulhanek, D.K., Weaver, F.M., and Majewski, W., 2011, Progressive Cenozoic cooling and the demise of Antarctica's last refugium: Proceedings of the National Academy of Sciences of the United States of America, v. 108, no. 28, p. 11,356–11,360, https://doi.org/10.1073/pnas.1014885108.
Anderson, J.B., Simkins, L.M., Bart, P.J., De Santis, L., Halberstadt, A.R.W., Olivo, E., and Greenwood, S.L., 2019, Seismic and geomorphic records of Antarctic ice sheet evolution in the Ross Sea and controlling factors in its behavior, in Le Heron, D.P., Hogan, K.A., Phillips, E.R., Huuse, M., Busfield, M.W., and Graham, A.G.C., eds., Glaciated Margins: The Sedimentary and Geophysical Archive: Geological Society [London] Special Publication 475, p. 223–240, https://doi.org/10.1144/SP475.5.
Balshaw-Biddle, K.M., 1981, Antarctic Glacial Chronology Reflected in the Oligocene through Pliocene Sedimentary Section in the Ross Sea [Ph.D. thesis]: Houston, Texas, Rice University, 140 p.
Barrett, P.J., 1986, Antarctic Cenozoic History from the MSSTS-1 Drillhole, McMurdo Sound: Department of Scientific and Industrial Research (New Zealand) Bulletin, v. 237, p. 241–251.
Bart, P.J., 2003, Were West Antarctic Ice Sheet grounding events in the Ross Sea a consequence of East Antarctic Ice Sheet expansion during the middle Miocene?: Earth and Planetary Science Letters, v. 216, no. 1-2, p. 93–107.
Bart, P.J., and Iwai, M., 2012, The overdeepening hypothesis: How erosional modification of the marine-scape during the early Antarctic Peninsula's Pacific margin: Palaeogeography, Palaeoclimatology, Palaeoecology, v. 335–336, p. 42–51, https://doi.org/10.1016/j.palaeo.2011.06.010.
Bart, P., Anderson, J., Trincardi, F., and Shipp, S., 2000, Seismic data from the Northern basin, Ross Sea, record extreme expansions of the East Antarctic Ice Sheet during the late Neogene: Marine Geology, v. 166, no. 1-4, p. 31–50, https://doi.org/10.1016/S0025-3227(00)00006-2.
Batchelor, C., Dowdeswell, J., and Pietras, J., 2013, Variable history of Quaternary ice-sheet advance across the Beaufort Sea margin, Arctic Ocean: Geology, v. 41, no. 2, p. 131–134, https://doi.org/10.1130/G33669.1.

Berger, A.L., Gulick, S.P.S., Spotila, J.A., Upton, P., Jaeger, J.M., Chapman, J.B., Worthington, L.A., Pavlis, T.L., Ridgway, K.D., Willems, B.A., and McAleer, R.J., 2008, Quaternary tectonic response to intensified glacial erosion in an orogenic wedge: Nature Geoscience, v. 1, no. 11, p. 793–799, https://doi.org/10.1038/ngeo334.
Bjarnadóttir, L.R., Winsborrow, M., and Andreassen, K., 2017, Large subglacial meltwater features in the central Barents Sea: Geology, v. 45, no. 2, p. 159–162, https://doi.org/10.1130/G38195.1.
Blankenship, D.D., Bentley, C.R., Rooney, S., and Alley, R.B., 1986, Seismic measurements reveal a saturated porous layer beneath an active Antarctic ice stream: Nature, v. 322, no. 6074, p. 54–57, https://doi.org/10.1038/322054a0.
Brancolini, G., Busetti, M., Coren, F., De Cillia, C., Marchetti, M., De Santis, L., Zanolla, C., Cooper, A., Cochrane, G., Zayatz, I., et al., 1995, ANTOSTRAT Project: Seismic stratigraphic atlas of the Ross Sea, Antarctica, in Cooper, A.K., Barker, P.F., and Brancolni, G., eds., Geology and Seismic Stratigraphy of the Antarctic Margin: American Geophysical Union Antarctic Research Series 68, p. A271–A286.
Cai, J., Powell, R.D., Cowan, E.A., and Carlson, P.R., 1997, Lithofacies and seismic-reflection interpretation of temperate glacimarine sedimentation in Tarr Inlet, Glacier Bay, Alaska: Marine Geology, v. 143, no. 1-4, p. 5–37, https://doi.org/10.1016/S0025-3227(97)00088-1.
Camerlenghi, A., Domack, E., Rebesco, M., Gilbert, R., Ishman, S., Leventer, A., Brachfeld, S., and Drake, A., 2001, Glacial morphology and post-glacial contourites in northern Prince Gustav Channel (NW Weddell Sea, Antarctica): Marine Geophysical Researches, v. 22, no. 5-6, p. 417–443, https://doi.org/10.1023/A:1016399616365.
Carlson, P.R., 1989, Seismic reflection characteristics of glacial and glacimarine sediment in the Gulf of Alaska and adjacent fjords: Marine Geology, v. 85, no. 2-4, p. 391–416, https://doi.org/10.1016/0025-3227(89)90161-8.
Close, D., 2010, Slope and fan deposition in deep-water turbidite systems, East Antarctica: Marine Geology, v. 274, no. 1-4, p. 21–31, https://doi.org/10.1016/j.margeo.2010.03.002.
Close, D., Stagg, H., and O'Brien, P., 2007, Seismic stratigraphy and sediment distribution on the Wilkes Land and Terre Adélie margins, East Antarctica: Marine Geology, v. 239, no. 1-2, p. 33–57, https://doi.org/10.1016/j.margeo.2006.12.010.
Conway, H., Hall, B., Denton, G., Gades, A., and Waddington, E., 1999, Past and future grounding-line retreat of the West Antarctic Ice Sheet: Science, v. 286, no. 5438, p. 280–283, https://doi.org/10.1126/science.286.5438.280.
Cooper, A.K., and O'Brien, P.E., 2004, Leg 188 synthesis: Transitions in the glacial history of the Prydz Bay region, East Antarctica, from ODP drilling, in Cooper, A.K., O'Brien, P.E., and Richter, C., eds., Proceedings of the Ocean Drilling Program, Scientific Results Volume 188: College Station, Texas, Ocean Drilling Program, p. 1–42.
De Angelis, H., and Skvarca, P., 2003, Glacier surge after ice shelf collapse: Science, v. 299, no. 5612, p. 1560–1562.
DeConto, R.M., and Pollard, D., 2016, Contribution of Antarctica to past and future sea-level rise: Nature, v. 531, no. 7596, p. 591–597, https://doi.org/10.1038/nature17145.
Denton, G.H., and Sugden, D.E., 2005, Meltwater features that suggest Miocene ice-sheet overriding of the Transantarctic Mountains in Victoria Land, Antarctica: Geografiska Annaler, ser. A, Physical Geography, v. 87, no. 1, p. 67–85, https://doi.org/10.1111/j.0435-3676.2005.00245.x.
De Santis, L., Anderson, J.B., Brancolini, G., and Zayatz, I., 1997, Seismic record of late Oligocene through Miocene glaciation on the central and eastern continental shelf of the Ross Sea, in Cooper, A.K., Barker, P.F., and Brancolni, G., eds., Geology and Seismic Stratigraphy of the Antarctic Margin: American Geophysical Union Antarctic Research Series 68, p. 235–260.
De Santis, L., Prato, S., Brancolini, G., Lovo, M., and Torelli, L., 1999, The Eastern Ross Sea continental shelf

during the Cenozoic: Implications for the West Antarctic Ice Sheet development: Global and Planetary Change, v. 23, no. 1-4, p. 173–196, https://doi.org/10.1016/S0921-8181(99)00056-9.

De Santis, L., Brancolini, G., and Donda, F., 2003, Seismo-stratigraphic analysis of the Wilkes Land continental margin (East Antarctica): Influence of glacially driven processes on the Cenozoic deposition: Deep-Sea Research II: Topical Studies in Oceanography, v. 50, no. 8-9, p. 1563–1594, https://doi.org/10.1016/S0967-0645(03)00079-1.

Domack, E., Amblas, D., Gilbert, R., Brachfeld, S., Camerlenghi, A., Rebesco, M., Canals, M., and Urgeles, R., 2006, Subglacial morphology and glacial evolution of the Palmer Deep outlet system, Antarctic Peninsula: Geomorphology, v. 75, no. 1-2, p. 125–142, https://doi.org/10.1016/j.geomorph.2004.06.013.

Donda, F., O'Brien, P., De Santis, L., Rebesco, M., and Brancolini, G., 2008, Mass wasting processes in the western Wilkes Land margin: Possible implications for East Antarctic glacial history: Palaeogeography, Palaeoclimatology, Palaeoecology, v. 260, no. 1-2, p. 77–91, https://doi.org/10.1016/j.palaeo.2007.08.008.

Dowdeswell, J.A., Ottesen, D., Rise, L., and Craig, J., 2007, Identification and preservation of landforms diagnostic of past ice-sheet activity on continental shelves from three-dimensional seismic evidence: Geology, v. 35, no. 4, p. 359–362, https://doi.org/10.1130/G23200A.1.

Dowdeswell, J.A., Cofaigh, C.Ó., Noormets, R., Larter, R.D., Hillenbrand, C.D., Benetti, S., Evans, J., and Pudsey, C., 2008, A major trough-mouth fan on the continental margin of the Bellingshausen Sea, West Antarctica: The Belgica Fan: Marine Geology, v. 252, no. 3-4, p. 129–140, https://doi.org/10.1016/j.margeo.2008.03.017.

Dowdeswell, J.A., Hogan, K., Cofaigh, C.Ó., Fugelli, E., Evans, J., and Noormets, R., 2014, Late Quaternary ice flow in a West Greenland fjord and cross-shelf trough system: Submarine landforms from Rink Isbrae to Uummannaq shelf and slope: Quaternary Science Reviews, v. 92, p. 292–309, https://doi.org/10.1016/j.quascirev.2013.09.007.

Dowdeswell, J.A., Canals, M., Jakobsson, M., Todd, B., Dowdeswell, E.K., and Hogan, K., 2016, The variety and distribution of submarine glacial landforms and implications for ice-sheet reconstruction, *in* Dowdeswell, J.A., et al., eds., Atlas of Submarine Glacial Landforms: Geological Society [London] Memoir 46, p. 519–552.

Drewry, D.J., 1976, Sedimentary basins of the East Antarctic craton from geophysical evidence: Tectonophysics, v. 36, no. 1-3, p. 301–314, https://doi.org/10.1016/0040-1951(76)90023-8.

Drewry, D., and Meldrum, D., 1978, Antarctic airborne radio echo sounding, 1977–78: The Polar Record, v. 19, no. 120, p. 267–273, https://doi.org/10.1017/S0032247400018271.

Eittreim, S., and Smith, G., 1987, Seismic sequences and their distribution on the Wilkes Land margin, *in* Eittreim, S., and Hampton, M.A., eds., The Antarctic Continental Margin: Geology and Geophysics of Offshore Wilkes Land: Circum-Pacific Council for Energy and Mineral Resources Earth Science Series 5A, p. 15–43.

Eittreim, S.L., Cooper, A.K., and Wannesson, J., 1995, Seismic stratigraphic evidence of ice-sheet advances on the Wilkes Land margin of Antarctica: Sedimentary Geology, v. 96, no. 1-2, p. 131–156, https://doi.org/10.1016/0037-0738(94)00130-M.

Elmore, C.R., Gulick, S.P., Willems, B., and Powell, R., 2013, Seismic stratigraphic evidence for glacial expanse during glacial maxima in the Yakutat Bay region, Gulf of Alaska: Geochemistry Geophysics Geosystems, v. 14, no. 4, p. 1294–1311, https://doi.org/10.1002/ggge.20097.

Escutia, C., Eittreim, S., Cooper, A., and Nelson, C., 2000, Morphology and acoustic character of the Antarctic Wilkes Land turbidite systems: Ice-sheet–sourced versus river-sourced fans: Journal of Sedimentary Research, v. 70, no. 1, p. 84–93, https://doi.org/10.1306/2DC40900-0E47-11D7-8643000102C1865D.

Escutia, C., Warnke, D., Acton, G., Barcena, A., Burckle, L., Canals, M., and Frazee, C., 2003, Sediment distribution and sedimentary processes across the Antarctic Wilkes Land margin during the Quaternary: Deep-Sea Research II: Topical Studies in Oceanography, v. 50, no. 8-9, p. 1481–1508, https://doi.org/10.1016/S0967-0645(03)00073-0.

Escutia, C., De Santis, L., Donda, F., Dunbar, R., Cooper, A., Brancolini, G., and Eittreim, S., 2005, Cenozoic ice sheet history from East Antarctic Wilkes Land continental margin sediments: Global and Planetary Change, v. 45, no. 1-3, p. 51–81, https://doi.org/10.1016/j.gloplacha.2004.09.010.

Escutia, C., Brinkhuis, H., and Klaus, A., and the IODP Expedition 318 Scientists, 2011, IODP Expedition 318: From greenhouse to icehouse at the Wilkes Land Antarctic margin: Scientific Drilling, v. 12, p. 15–23, https://doi.org/10.5194/sd-12-15-2011.

Evans, J., Pudsey, C.J., Ó Cofaigh, C., Morris, P., and Domack, E., 2005, Late Quaternary glacial history, flow dynamics and sedimentation along the eastern margin of the Antarctic Peninsula ice sheet: Quaternary Science Reviews, v. 24, no. 5-6, p. 741–774, https://doi.org/10.1016/j.quascirev.2004.10.007.

Exon, N., Kennett, J., Malone, M., Brinkhuis, H., Chaproniere, G., Ennyu, A., Fothergill, P., Fuller, M., Grauert, M., Hill, P., Janecek, T., Kelly, C., Latimer, J., McGonigal, K., Nees, S., Ninnemann, U., Nuernberg, D., Pekar, S., Pellaton, C., Pfuhl, H., Robert, C., Rohl, U., Schellenberg, S., Shevenell, A., Stickley, C., Suzuki, N., Touchard, Y., Wei, W., and White, T., 2002, Drilling reveals climatic consequences of Tasmanian Gateway opening: Eos (Washington, D.C.), v. 83, no. 23, p. 253–259, https://doi.org/10.1029/2002EO000176.

Fernandez, R., Gulick, S., Domack, E., Montelli, A., Leventer, A., Shevenell, A., Frederick, B., and NBP1402 Science Party, 2018, Past ice stream and ice sheet changes on the continental shelf off the Sabrina Coast, East Antarctica: Geomorphology, v. 317, p. 10–22, https://doi.org/10.1016/j.geomorph.2018.05.020.

Florindo, F., and Siegert, M.J., 2009, Antarctic Climate Evolution: Elsevier, 606 p.

Flower, B.P., and Kennett, J.P., 1994, The middle Miocene climatic transition: East Antarctic Ice Sheet development, deep ocean circulation and global carbon cycling: Palaeogeography, Palaeoclimatology, Palaeoecology, v. 108, no. 3-4, p. 537–555, https://doi.org/10.1016/0031-0182(94)90251-8.

Francis, J., 1999, Evidence from fossil plants for Antarctic palaeoclimates over the past 100 million years: Terra Antarctica Report 3, p. 43–52.

Francis, J.E., 2000, Fossil wood from Eocene high latitude forests: McMurdo Sound, Antarctica, *in* Stilwell, J.D., and Feldmann, R.M., eds., Paleobiology and Paleoenvironments of Eocene Rocks: McMurdo Sound: East Antarctica: American Geophysical Union Antarctic Research Series 76, p. 253–260.

Francis, J., Marenssi, S., Levy, R., Hambrey, M., Thorn, V., Mohr, B., Brinkhuis, H., Warnaar, J., Zachos, J., Bohaty, S., and DeConto, R., 2008, From greenhouse to icehouse—The Eocene/Oligocene in Antarctica, *in* Florindo, F., and Siegert, M., eds., Antarctic Climate Evolution: Elsevier, Developments in Earth and Environmental Sciences 8, p. 309–368, https://doi.org/10.1016/S1571-9197(08)00008-6.

Fretwell, P., Pritchard, H.D., Vaughan, D.G., Bamber, J.L., Barrand, N.E., Bell, R., Bianchi, C., Bingham, R.G., Blankenship, D.D., Casassa, G., Catania, G., Callens, D., Conway, H., Cook, A.J., Corr, H.F.J., Damaske, D., Damm, V., Ferraccioli, F., Forsberg, R., Fujita, Y., Gim, Y., Gogineni, P., Griggs, J.A., Hindmarsh, R.C.A., Holmlund, P., Holt, J.W., Jacobel, R.W., Jenkins, A., Jokat, W., Jordan, T., King, E.C., Kohler, J., Krabill, W., Riger-Kusk, M., Langley, K.A., Leitchenkov, G., Leuschen, C., Luyendyk, B.P., Matsuoka, K., Mouginot, J., Nitsche, F.O., Nogi, Y., Nost, O.A., Popov, S.V., Rignot, E., Rippin, D.M., Rivera, A., Roberts, J., Ross, N., Siegert, M.J., Smith, A.M., Steinhage, D., Studinger, M., Sun, B., Tinto, B.K., Welch, B.C., Wilson, D., Young, D.A., Xiangbin, C., and Zirizzotti, A., 2012, Bedmap2: Improved ice bed, surface and thickness datasets for Antarctica: The Cryosphere Discussions, v. 6, p. 4305–4361, https://doi.org/10.5194/tcd-6-4305-2012.

Gasson, E., DeConto, R.M., Pollard, D., and Levy, R.H., 2016, Dynamic Antarctic ice sheet during the early to mid-Miocene: Proceedings of the National Academy of Sciences of the United States of America, v. 113, no. 13, p. 3459–3464, https://doi.org/10.1073/pnas.1516130113.

Gohl, K., Uenzelmann-Neben, G., Larter, R.D., Hillenbrand, C.D., Hochmuth, K., Kalberg, T., Weigelt, E., Davy, B., Kuhn, G., and Nitsche, F.O., 2013, Seismic stratigraphic record of the Amundsen Sea Embayment shelf from pre-glacial to recent times: Evidence for a dynamic West Antarctic Ice Sheet: Marine Geology, v. 344, p. 115–131, https://doi.org/10.1016/j.margeo.2013.06.011.

Golledge, N.R., Fogwill, C.J., Mackintosh, A.N., and Buckley, K.M., 2012, Dynamics of the Last Glacial Maximum Antarctic ice-sheet and its response to ocean forcing: Proceedings of the National Academy of Sciences of the United States of America, v. 109, no. 40, p. 16,052–16,056, https://doi.org/10.1073/pnas.1205385109.

Golledge, N.R., Kowalewski, D.E., Naish, T.R., Levy, R.H., Fogwill, C.J., and Gasson, E.G., 2015, The multimillennial Antarctic commitment to future sea-level rise: Nature, v. 526, no. 7573, p. 421, https://doi.org/10.1038/nature15706.

Golledge, N., Levy, R., McKay, R., and Naish, T., 2017, East Antarctic Ice Sheet most vulnerable to Weddell Sea warming: Geophysical Research Letters, v. 44, no. 5, p. 2343–2351, https://doi.org/10.1002/2016GL072422.

Graham, A.G., Larter, R.D., Gohl, K., Hillenbrand, C.D., Smith, J.A., and Kuhn, G., 2009, Bedform signature of a West Antarctic palaeo–ice stream reveals a multi-temporal record of flow and substrate control: Quaternary Science Reviews, v. 28, no. 25-26, p. 2774–2793, https://doi.org/10.1016/j.quascirev.2009.07.003.

Greenbaum, J., Blankenship, D., Young, D., Richter, T., Roberts, J., Aitken, A., Legresy, B., Schroeder, D., Warner, R., Van Ommen, T., and Siegert, M.J., 2015, Ocean access to a cavity beneath Totten Glacier in East Antarctica: Nature Geoscience, v. 8, no. 4, p. 294–298, https://doi.org/10.1038/ngeo2388.

Greene, C.A., Blankenship, D.D., Gwyther, D.E., Silvano, A., and van Wijk, E., 2017, Wind causes Totten ice shelf melt and acceleration: Science Advances, v. 3, no. 11, p. e1701681, https://doi.org/10.1126/sciadv.1701681.

Gulick, S.P., Shevenell, A.E., Montelli, A., Fernandez, R., Smith, C., Warny, S., Bohaty, S.M., Sjunneskog, C., Leventer, A., Frederick, B., and Blankenship, D.D., 2017, Initiation and long-term instability of the East Antarctic Ice Sheet: Nature, v. 552, no. 7684, p. 225–229, https://doi.org/10.1038/nature25026.

Hambrey, M.J., Ehrmann, W., and Larsen, B., 1991, Cenozoic glacial record of the Prydz Bay continental shelf, East Antarctica, *in* Barron, J., and Larsen, B., et al., Proceedings of the Ocean Drilling Program, Scientific Results Volume 119: College Station, Texas, Ocean Drilling Program, p. 77–132, https://doi.org/10.2973/odp.proc.sr.119.200.1991.

Hayes, D., 1975, General synthesis, Deep Sea Drilling Project Leg 28, *in* Initial Reports of the Deep Sea Drilling Project Volume 28: Washington, D.C., U.S. Government Printing Office, p. 919–942, https://doi.org/10.2973/dsdp.proc.28.136.1975.

Hein, A.S., Fogwill, C.J., Sugden, D.E., and Xu, S., 2011, Glacial/interglacial ice-stream stability in the Weddell Sea Embayment, Antarctica: Earth and Planetary Science Letters, v. 307, no. 1-2, p. 211–221, https://doi.org/10.1016/j.epsl.2011.04.037.

Herbert, T.D., Lawrence, K.T., Tzanova, A., Peterson, L.C., Caballero-Gill, R., and Kelly, C.S., 2016, Late Miocene global cooling and the rise of modern ecosystems: Nature Geoscience, v. 9, no. 11, p. 843, https://doi.org/10.1038/ngeo2813.

Huuse, M., and Lykke-Andersen, H., 2000, Overdeepened Quaternary valleys in the eastern Danish North Sea: Morphology and origin: Quaternary Science Reviews, v. 19, no. 12, p. 1233–1253, https://doi.org/10.1016/S0277-3791(99)00103-1.

Iwai, M., and Winter, D., 2002, Data report: Taxonomic notes of Neogene diatoms from the western Antarctic Peninsula: Ocean Drilling Program Leg 178, *in* Barker, P.F., Camerlenghi, A., et al., eds., Proceedings of the Ocean Drilling Program, Scientific Results Volume 178: College Station, Texas, Ocean Drilling Program, p. 1–57.

Kennett, J.P., 1977, Cenozoic evolution of Antarctic glaciation, the circum–Antarctic Ocean, and their impact on global paleoceanography: Journal of Geophysical Research, v. 82, no. 27, p. 3843–3860, https://doi.org/10.1029/JC082i027p03843.

Kennett, J.P., and Shackleton, N.J., 1976, Oxygen isotopic evidence for the development of the psychrosphere 38 Myr ago: Nature, v. 260, no. 5551, p. 513–515, https://doi.org/10.1038/260513a0.

Kingslake, J., Scherer, R., Albrecht, T., Coenen, J., Powell, R., Reese, R., Stansell, N., Tulaczyk, S., Wearing, M., and Whitehouse, P., 2018, Extensive retreat and re-advance of the West Antarctic Ice Sheet during the Holocene: Nature, v. 558, no. 7710, p. 430–434, https://doi.org/10.1038/s41586-018-0208-x.

Kominz, M., Browning, J., Miller, K., Sugarman, P., Mizintseva, S., and Scotese, C., 2008, Late Cretaceous to Miocene sea-level estimates from the New Jersey and Delaware coastal plain coreholes: An error analysis: Basin Research, v. 20, no. 2, p. 211–226, https://doi.org/10.1111/j.1365-2117.2008.00354.x.

Kristensen, T.B., Piotrowski, J.A., Huuse, M., Clausen, O.R., and Hamberg, L., 2008, Time-transgressive tunnel valley formation indicated by infill sediment structure, North Sea—The role of glaciohydraulic supercooling: Earth Surface Processes and Landforms, v. 33, no. 4, p. 546–559.

Kuvaas, B., and Kristoffersen, Y., 1991, The Crary Fan: A trough-mouth fan on the Weddell Sea continental margin, Antarctica: Marine Geology, v. 97, no. 3-4, p. 345–362, https://doi.org/10.1016/0025-3227(91)90125-N.

Larter, R.D., Anderson, J.B., Graham, A.G., Gohl, K., Hillenbrand, C.D., Jakobsson, M., Johnson, J.S., Kuhn, G., Nitsche, F.O., Smith, J.A., Witus, A.E., Bentley, M.J., Dowdeswell, J.A., Ehrmann, W., Klages, J.P., Lindow, J., Ó Cofaigh, C., and Spiegel, C., 2014, Reconstruction of changes in the Amundsen Sea and Bellingshausen Sea sector of the West Antarctic Ice Sheet since the Last Glacial Maximum: Quaternary Science Reviews, v. 100, p. 55–86, https://doi.org/10.1016/j.quascirev.2013.10.016.

Lawver, L.A., and Gahagan, L.M., 2003, Evolution of Cenozoic seaways in the circum-Antarctic region: Palaeogeography, Palaeoclimatology, Palaeoecology, v. 198, no. 1-2, p. 11–37, https://doi.org/10.1016/S0031-0182(03)00392-4.

Levy, R., Harwood, D., Florindo, F., Sangiorgi, F., Tripati, R., Von Eynatten, H., Gasson, E., Kuhn, G., Tripati, A., DeConto, R., Fielding, C., Field, B., Golledge, N., McKay, R., Naish, T., Olney, M., Pollard, D., Schouten, S., Talarico, F., Warny, S., Willmott, V., Acton, G., Panter, K., Paulsen, T., Taviani, M., and SMS Science Team, 2016, Antarctic ice sheet sensitivity to atmospheric CO_2 variations in the early to mid-Miocene: Proceedings of the National Academy of Sciences of the United States of America, v. 113, no. 13, p. 3453–3458, https://doi.org/10.1073/pnas.1516030113.

Lewis, A.R., Marchant, D.R., Kowalewski, D.E., Baldwin, S.L., and Webb, L.E., 2006, The age and origin of the Labyrinth, western Dry Valleys, Antarctica: Evidence for extensive middle Miocene subglacial floods and freshwater discharge to the Southern Ocean: Geology, v. 34, no. 7, p. 513–516, https://doi.org/10.1130/G22145.1.

Lewis, A.R., Marchant, D.R., Ashworth, A.C., Hedenäs, L., Hemming, S.R., Johnson, J.V., Leng, M.J., Machlus, M.L., Newton, A.E., Raine, J.I., Willenbring, J.K., Williams, M., and Wolfe, A.P., 2008, Mid-Miocene cooling and the extinction of tundra in continental Antarctica: Proceedings of the National Academy of Sciences of the United States of America, v. 105, no. 31, p. 10,676–10,680, https://doi.org/10.1073/pnas.0802501105.

Livingstone, S.J., and Clark, C.D., 2016, Morphological properties of tunnel valleys of the southern sector of the Laurentide ice sheet and implications for their formation: Earth Surface Dynamics, v. 4, p. 567–589, https://doi.org/10.5194/esurf-4-567-2016.

Livingstone, S.J., Cofaigh, C.Ó, Stokes, C.R., Hillenbrand, C.D., Vieli, A., and Jamieson, S.S., 2012, Antarctic palaeo–ice streams: Earth-Science Reviews, v. 111, no. 1-2, p. 90–128, https://doi.org/10.1016/j.earscirev.2011.10.003.

Lonergan, L., Maidment, S.C., and Collier, J.S., 2006, Pleistocene subglacial tunnel valleys in the central North Sea basin: 3-D morphology and evolution: Journal of Quaternary Science, v. 21, no. 8, p. 891–903, https://doi.org/10.1002/jqs.1015.

Lowe, A.L., and Anderson, J.B., 2002, Reconstruction of the West Antarctic Ice Sheet in Pine Island Bay during the Last Glacial Maximum and its subsequent retreat history: Quaternary Science Reviews, v. 21, no. 16-17, p. 1879–1897, https://doi.org/10.1016/S0277-3791(02)00006-9.

Lowe, A.L., and Anderson, J.B., 2003, Evidence for abundant subglacial meltwater beneath the paleo–ice sheet in Pine Island Bay, Antarctica: Journal of Glaciology, v. 49, no. 164, p. 125–138, https://doi.org/10.3189/172756503781830971.

Mackintosh, A.N., Verleyen, E., O'Brien, P.E., White, D.A., Jones, R.S., McKay, R., Dunbar, R., Gore, D.B., Fink, D., Post, A.L., Miura, H., Leventer, A., Goodwin, I., Hodgson, D.A., Lilly, K., Crosta, X., Golledge, N.R., Wagner, B., and Masse, G., 2014, Retreat history of the East Antarctic Ice Sheet since the Last Glacial Maximum: Quaternary Science Reviews, v. 100, p. 10–30, https://doi.org/10.1016/j.quascirev.2013.07.024.

McKay, R., Browne, G., Carter, L., Cowan, E., Dunbar, G., Krissek, L., Naish, T., Powell, R., Reed, J., Talarico, F., and Wilch, T., 2009, The stratigraphic signature of the late Cenozoic Antarctic ice sheets in the Ross Embayment: Geological Society of America Bulletin, v. 121, no. 11-12, p. 1537–1561, https://doi.org/10.1130/B26540.1.

McKay, R.M., Barrett, P., Levy, R., Naish, T., Golledge, N., and Pyne, A., 2016, Antarctic Cenozoic climate history from sedimentary records: ANDRILL and beyond: Philosophical Transactions of the Royal Society, ser. A, Mathematical, Physical and Engineering Sciences, v. 374, no. 2059, p. 20140301, https://doi.org/10.1098/rsta.2014.0301.

McKay, R.M., De Santis, L., Kulhanek, D.K., Ash, J.A., Beny, F., Browne, I.M., Cortese, G., De Sousa, I.M.C., Dodd, J.D., Esper, O.E., Gales, J.G., Harwood, D.H., Ishino, S., Keisling, B.K., Kim, S., Kim, S., Laberg, J.S., Leckie, R.M., Müller, J., Patterson, M.P., Romans, B.R., Romero, O.R., Sangiorgi, F., Seki, O., Powell, J.P., Shevenell, A., Singh, S.S., Sugisaki, S., Van De Flierdt, T., Van Peer, T.E., Xiao, W., and Xiong, Z., 2018, Ross Sea West Antarctic Ice Sheet history: Ocean-ice sheet interactions and West Antarctic Ice Sheet vulnerability: Clues from the Neogene and Quaternary record of the outer Ross Sea continental margin, in International Ocean Discovery Program Expedition 374 Preliminary Report: International Ocean Discovery Program, https://doi.org/10.14379/iodp.pr.374.2018.

Miller, K.G., Kominz, M.A., Browning, J.V., Wright, J.D., Mountain, G.S., Katz, M.E., Sugarman, P.J., Cramer, B.S., Christie-Blick, N., and Pekar, S.F., 2005, The Phanerozoic record of global sea-level change: Science, v. 310, no. 5752, p. 1293–1298, https://doi.org/10.1126/science.1116412.

Mohajerani, Y., Velicogna, I., and Rignot, E., 2018, Mass loss of Totten and Moscow University glaciers, East Antarctica, using regionally optimized GRACE mascons: Geophysical Research Letters, v. 45, no. 14, p. 7010–7018, https://doi.org/10.1029/2018GL078173.

Montelli, A., Gulick, S.P., Worthington, L.L., Mix, A., Davies-Walczak, M., Zellers, S.D., and Jaeger, J.M., 2017, Late Quaternary glacial dynamics and sedimentation variability in the Bering Trough, Gulf of Alaska: Geology, v. 45, no. 3, p. 251–254, https://doi.org/10.1130/G38836.1.

Mudelsee, M., Bickert, T., Lear, C.H., and Lohmann, G., 2014, Cenozoic climate changes: A review based on time series analysis of marine benthic δ18O records: Reviews of Geophysics, v. 52, no. 3, p. 333–374, https://doi.org/10.1002/2013RG000440.

Naish, T.R., Woolfe, K.J., Barrett, P.J., Wilson, G.S., Atkins, C., Bohaty, S.M., Bücker, C.J., Claps, M., Davey, F.J., Dunbar, G.B., Dunn, A.G., Fielding, C.R., Florindo, F., Hannah, M.J., Harwood, D.M., Henrys, S.A., Krissek, L.A., Lavelle, M., van der Meer, J., McIntosh, W.C., Niessen, F., Passchier, S., Powell, R.D., Roberts, A.P., Sagnotti, L., Scherer, R.P., Strong, C.P., Talarico, F., Verosub, K.L., Villa, G., Watkins, D.K., Webb, P.-N., and Wonik, T., 2001, Orbitally induced oscillations in the East Antarctic Ice Sheet at the Oligocene/Miocene boundary: Nature, v. 413, no. 6857, p. 719–723, https://doi.org/10.1038/35099534.

Naish, T.R., Powell, R., Levy, R., Wilson, G., Scherer, R., Talarico, F., Krissek, L., Niessen, F., Pompilio, M., Wilson, T., Carter, L., DeConto, R., Huybers, P., McKay, R., Pollard, D., Ross, J., Winter, D., Barrett, P., Browne, G., Cody, R., Cowan, E., Crampton, J., Dunbar, G., Dunbar, N., Florindo, F., Gebhardt, C., Graham, I., Hannah, M., Hansaraj, D., Harwood, D., Helling, D., Henrys, S., Hinnov, L., Kuhn, G., Kyle, P., Läufer, A., Maffioli, P., Magens, D., Mandernack, K., McIntosh, W., Millan, C., Morin, R., Ohneiser, C., Paulsen, T., Persico, D., Raine, I., Reed, J., Riesselman, C., Sagnotti, L., Schmitt, D., Sjunneskog, C., Strong, P., Taviani, M., Vogel, S., Wilch, T., and Williams, T., 2009, Obliquity-paced Pliocene West Antarctic Ice Sheet oscillations: Nature, v. 458, no. 7236, p. 322–328, https://doi.org/10.1038/nature07867.

Nitsche, F.O., Gohl, K., Larter, R.D., Hillenbrand, C.D., Kuhn, G., Smith, J., Jacobs, S.S., Anderson, J., and Jakobsson, M., 2013, Paleo ice flow and subglacial meltwater dynamics in Pine Island Bay, West Antarctica: The Cryosphere, v. 7, p. 249–262, https://doi.org/10.5194/tc-7-249-2013.

Nývlt, D., Košler, J., Mlcoch, B., Mixa, P., Lisá, L., Bubík, M., and Hendriks, B.W., 2011, The Mendel Formation: Evidence for late Miocene climatic cyclicity at the northern tip of the Antarctic Peninsula: Palaeogeography, Palaeoclimatology, Palaeoecology, v. 299, no. 1-2, p. 363–384, https://doi.org/10.1016/j.palaeo.2010.11.017.

Nývlt, D., Braucher, R., Engel, Z., Mlcoch, B., Team A, et al., 2014, Timing of the northern Prince Gustav ice stream retreat and the deglaciation of northern James Ross Island, Antarctic Peninsula, during the last glacial–interglacial transition: Quaternary Research, v. 82, no. 2, p. 441–449, https://doi.org/10.1016/j.yqres.2014.05.003.

O'Brien, P., and Harris, P., 1996, Patterns of glacial erosion and deposition in Prydz Bay and the past behaviour of the Lambert Glacier: Papers and Proceedings of the Royal Society of Tasmania, v. 130, p. 79–85, https://doi.org/10.26749/rstpp.130.2.79.

O'Brien, P., Cooper, A., Richter, C., Baldauf, J., and Richter, C., 2001, Initial Reports, Prydz Bay–Cooperation Sea, Antarctica: Glacial history and paleoceanography, in Proceedings Ocean Drilling Program, Initial Reports Volume 88: College Station Texas, Texas A&M University.

Ó Cofaigh, C., 1996, Tunnel valley genesis: Progress in Physical Geography, v. 20, no. 1, p. 1–19, https://doi.org/10.1177/030913339602000101.

Ó Cofaigh, C., Pudsey, C.J., Dowdeswell, J.A., and Morris, P., 2002, Evolution of subglacial bedforms along a paleo–ice stream, Antarctic Peninsula continental shelf: Geophysical Research Letters, v. 29, no. 8, p. 41-1–41-4, https://doi.org/10.1029/2001GL014488.

Pälike, H., Norris, R.D., Herrle, J.O., Wilson, P.A., Coxall, H.K., Lear, C.H., Shackleton, N.J., Tripati, A.K., and Wade, B.S., 2006, The heartbeat of the Oligocene climate system: Science, v. 314, no. 5807, p. 1894–1898, https://doi.org/10.1126/science.1133822.

Passchier, S., Browne, G., Field, B., Fielding, C., Krissek, L., Panter, K., Pekar, S., and Team, A.S.S., 2011, Early and middle Miocene Antarctic glacial history from the sedimentary facies distribution in the AND-2A drill hole, Ross Sea, Antarctica: Geological Society of America Bulletin, v. 123, no. 11-12, p. 2352–2365, https://doi.org/10.1130/B30334.1.

Piotrowski, J.A., 1997, Subglacial hydrology in north-western Germany during the last glaciation: Groundwater flow, tunnel valleys and hydrological cycles: Quaternary Science Reviews, v. 16, no. 2, p. 169–185, https://doi.org/10.1016/S0277-3791(96)00046-7.

Powell, R.D., and Cooper, J.M., 2002, A glacial sequence stratigraphic model for temperate, glaciated continental shelves, in Dowdeswell, J.A., and Ó Cofaigh, C., eds., Glacier-Influenced Sedimentation on High-Latitude Continental Margins: Geological Society [London] Special Publication 203, p. 215–244, https://doi.org/10.1144/GSL.SP.2002.203.01.12.

Praeg, D., 2003, Seismic imaging of mid-Pleistocene tunnel-valleys in the North Sea Basin—High resolution from low frequencies: Journal of Applied Geophysics, v. 53, no. 4, p. 273–298, https://doi.org/10.1016/j.jappgeo.2003.08.001.

Pritchard, H.D., Arthern, R.J., Vaughan, D.G., and Edwards, L.A., 2009, Extensive dynamic thinning on the margins of the Greenland and Antarctic ice sheets: Nature, v. 461, no. 7266, p. 971–975, https://doi.org/10.1038/nature08471.

Rebesco, M., Larter, R.D., Barker, P.F., Camerlenghi, A., and Vanneste, L.E., 1997, The history of sedimentation on the continental rise west of the Antarctic Peninsula, *in* Barker, P.F., and Cooper, A.K., eds., Geology and Seismic Stratigraphy of the Antarctic Margin 2: American Geophysical Union Antarctic Research Series 71, p. 29–49, https://doi.org/10.1029/AR071p0029.

Rebesco, M., Camerlenghi, A., and Zanolla, C., 1998, Bathymetry and morphogenesis of the continental margin west of the Antarctic Peninsula: Terra Antartica, v. 5, no. 4, p. 715–725.

Rebesco, M., Pudsey, C., Canals, M., Camerlenghi, A., Barker, P., Estrada, F., and Giorgetti, A., 2002, Sediment drifts and deep-sea channel systems, Antarctic Peninsula Pacific Margin, *in* Stow, D.A.V., Pudsey, C.J., Howe, J.A., Faugères, J.-C., and Viana, A.R., eds., Deep-water Contourite Systems: Modern Drifts and Ancient Series, Seismic and Sedimentary Characteristics: Geological Society [London] Memoir 22, p. 353–371.

Rignot, E., 1998, Fast recession of a West Antarctic glacier: Science, v. 281, no. 5376, p. 549–551, https://doi.org/10.1126/science.281.5376.549.

Rignot, E., Bamber, J.L., Van Den Broeke, M.R., Davis, C., Li, Y., Van De Berg, W.J., and Van Meijgaard, E., 2008, Recent Antarctic ice mass loss from radar interferometry and regional climate modelling: Nature Geoscience, v. 1, no. 2, p. 106–110, https://doi.org/10.1038/ngeo102.

Rignot, E., Mouginot, J., and Scheuchl, B., 2011, Ice flow of the Antarctic ice sheet: Science, v. 333, no. 6048, p. 1427–1430, https://doi.org/10.1126/science.1208336.

Rignot, E., Mouginot, J., Scheuchl, B., van den Broeke, M., van Wessem, M.J., and Morlighem, M., 2019, Four decades of Antarctic ice sheet mass balance from 1979–2017: Proceedings of the National Academy of Sciences of the United States of America, v. 116, no. 4, p. 1095–1103, https://doi.org/10.1073/pnas.1812883116.

Rintoul, S.R., Silvano, A., Pena-Molino, B., van Wijk, E., Rosenberg, M., Greenbaum, J.S., and Blankenship, D.D., 2016, Ocean heat drives rapid basal melt of the Totten ice shelf: Science Advances, v. 2, no. 12, p. e1601610, https://doi.org/10.1126/sciadv.1601610.

Roberts, J., Galton-Fenzi, B.K., Paolo, F.S., Donnelly, C., Gwyther, D.E., Padman, L., Young, D., Warner, R., Greenbaum, J., Fricker, H.A., Payne, A.J., Cornford, S., Le Brocq, A., van Ommen, T., Blankenship, D., and Siegert, M.J., 2018, Ocean forced variability of Totten Glacier mass loss, *in* Siegert, M.J., Jamieson, S.S.R., and White, D.A., eds., Exploration of Subsurface Antarctica: Uncovering Past Changes and Modern Processes: Geological Society [London] Special Publication 461, p. 175–186, https://doi.org/10.1144/SP461.6.

Sangiorgi, F., Bijl, P.K., Passchier, S., Salzmann, U., Schouten, S., McKay, R., Cody, R.D., Pross, J., Flierdt, T., Bohaty, S.M., Levy, R., Williams, T., Escutia, C., and Brinkhuis, H., 2018, Southern Ocean warming and Wilkes Land ice sheet retreat during the mid-Miocene: Nature Communications, v. 9, no. 1, p. 317, https://doi.org/10.1038/s41467-017-02609-7.

Scheuer, C., Gohl, K., Larter, R.D., Rebesco, M., and Udintsev, G., 2006, Variability in Cenozoic sedimentation along the continental rise of the Bellingshausen Sea, West Antarctica: Marine Geology, v. 227, no. 3-4, p. 279–298, https://doi.org/10.1016/j.margeo.2005.12.007.

Shaw, J., 2002, The meltwater hypothesis for subglacial bedforms: Quaternary International, v. 90, no. 1, p. 5–22, https://doi.org/10.1016/S1040-6182(01)00089-1.

Shevenell, A.E., Kennett, J.P., and Lea, D.W., 2004, Middle Miocene Southern Ocean cooling and Antarctic cryosphere expansion: Science, v. 305, no. 5691, p. 1766–1770, https://doi.org/10.1126/science.1100061.

Shevenell, A.E., Kennett, J.P., and Lea, D.W., 2008, Middle Miocene ice sheet dynamics, deep-sea temperatures, and carbon cycling: A Southern Ocean perspective: Geochemistry Geophysics Geosystems, v. 9, no. 2, Q02006, https://doi.org/10.1029/2007GC001736.

Shipp, S., Anderson, J., and Domack, E., 1999, Late Pleistocene–Holocene retreat of the West Antarctic Ice-Sheet system in the Ross Sea: Part 1—Geophysical results: Geological Society of America Bulletin, v. 111, no. 10, p. 1486–1516, https://doi.org/10.1130/0016-7606(1999)111<1486:LPHROT>2.3.CO;2.

Siegert, M.J., Taylor, J., and Payne, A.J., 2005, Spectral roughness of subglacial topography and implications for former ice-sheet dynamics in East Antarctica: Global and Planetary Change, v. 45, no. 1-3, p. 249–263, https://doi.org/10.1016/j.gloplacha.2004.09.008.

Siegert, M.J., Le Brocq, A., and Payne, A.J., 2007, Hydrological connections between Antarctic subglacial lakes, the flow of water beneath the East Antarctic Ice Sheet and implications for sedimentary processes, *in* Montanez, I., Hambrey, M.J., Christoffersen, P., Glasser, N.F., and Hubbard, B., eds., Glacial Sedimentary Processes and Products: International Association of Sedimentologists Special Publication 39, p. 3–10, https://doi.org/10.1002/9781444304435.ch1.

Simkins, L.M., Anderson, J.B., Greenwood, S.L., Gonnermann, H.M., Prothro, L.O., Halberstadt, A.R.W., Stearns, L.A., Pollard, D., and DeConto, R.M., 2017, Anatomy of a meltwater drainage system beneath the ancestral East Antarctic Ice Sheet: Nature Geoscience, v. 10, no. 9, p. 691–697, https://doi.org/10.1038/ngeo3012.

Smith, J.A., Hillenbrand, C.D., Larter, R.D., Graham, A.G., and Kuhn, G., 2009, The sediment infill of subglacial meltwater channels on the West Antarctic continental shelf: Quaternary Research, v. 71, no. 2, p. 190–200, https://doi.org/10.1016/j.yqres.2008.11.005.

Smith, R.T., and Anderson, J.B., 2010, Ice-sheet evolution in James Ross Basin, Weddell Sea margin of the Antarctic Peninsula: The seismic stratigraphic record: Geological Society of America Bulletin, v. 122, no. 5-6, p. 830–842, https://doi.org/10.1130/B26486.1.

Stewart, M., Lonergan, L., and Hampson, G., 2012, 3D seismic analysis of buried tunnel valleys in the Central North Sea: Tunnel valley fill sedimentary architecture, *in* Huuse, M., Redfern, J., Le Heron, D.P., Dixon, R.J., Moscariello, A., and Craig, J., eds., Glaciogenic Reservoirs and Hydrocarbon Systems: Geological Society [London] Special Publication 368, p. 173–184, https://doi.org/10.1144/SP368.9.

Stickley, C.E., Brinkhuis, H., Schellenberg, S.A., Sluijs, A., Röhl, U., Fuller, M., Grauert, M., Huber, M., Warnaar, J., and Williams, G.L., 2004, Timing and nature of the deepening of the Tasmanian Gateway: Paleoceanography, v. 19, no. 4, PA4027, https://doi.org/10.1029/2004PA001022.

Stocchi, P., Escutia, C., Houben, A.J., Vermeersen, B.L., Bijl, P.K., Brinkhuis, H., DeConto, R.M., Galeotti, S., Passchier, S., Pollard, D., Brinkhuis, H., Escutia, C., Klaus, A., Fehr, A., Williams, T., Bendle, J.A.P., Bijl, P.K., Bohaty, S.M., Carr, S.A., Dunbar, R.B., Flores, J.A., Gonzàlez, J.J., Hayden, T.G., Iwai, M., Jimenez-Espejo, F.J., Katsuki, K., Kong, G.S., McKay, R.M., Nakai, M., Olney, M.P., Passchier, S., Pekar, S.F., Pross, J., Riesselman, C., Röhl, U., Sakai, T., Shrivastava, P.K., Stickley, C.E., Sugisaki, S., Tauxe, L., Tuo, S., van de Flierdt, T., Welsh, K., and Yamane, M., 2013, Relative sea-level rise around East Antarctica during Oligocene glaciation: Nature Geoscience, v. 6, no. 5, p. 380–384, https://doi.org/10.1038/ngeo1783.

Sugden, D.E., Denton, G.H., and Marchant, D.R., 1995, Landscape evolution of the Dry Valleys, Transantarctic Mountains: Tectonic implications: Journal of Geophysical Research–Solid Earth, v. 100, no. B6, p. 9949–9968, https://doi.org/10.1029/94JB02875.

Taylor, J., Siegert, M.J., Payne, A., Hambrey, M.J., O'Brien, P., Cooper, A., and Leitchenkov, G., 2004, Topographic controls on post-Oligocene changes in ice-sheet dynamics, Prydz Bay region, East Antarctica: Geology, v. 32, no. 3, p. 197–200, https://doi.org/10.1130/G20275.1.

ten Brink, U.S., and Schneider, C., 1995, Glacial morphology and depositional sequences of the Antarctic continental shelf: Geology, v. 23, no. 7, p. 580–584, https://doi.org/10.1130/0091-7613(1995)023<0580:GMADSO>2.3.CO;2.

Uenzelmann-Neben, G., 2018, Variations in ice-sheet dynamics along the Amundsen Sea and Bellingshausen Sea West Antarctic Ice Sheet margin: Geological Society of America Bulletin, v. 131, no. 3-4, p. 479–498, https://doi.org/10.1130/B31744.1.

Uenzelmann-Neben, G., and Gohl, K., 2014, Early glaciation already during the early Miocene in the Amundsen Sea, southern Pacific: Indications from the distribution of sedimentary sequences: Global and Planetary Change, v. 120, p. 92–104, https://doi.org/10.1016/j.gloplacha.2014.06.004.

van der Vegt, P., Janszen, A., and Moscariello, A., 2012, Tunnel valleys: Current knowledge and future perspectives, *in* Huuse, M., Redfern, J., Le Heron, D.P., Dixon, R.J., Moscariello, A., and Craig, J., eds., Glaciogenic Reservoirs and Hydrocarbon Systems: Geological Society [London] Special Publication 368, p. 75–97, https://doi.org/10.1144/SP368.13.

Warny, S., Askin, R.A., Hannah, M.J., Mohr, B.A., Raine, J.I., Harwood, D.M., Florindo, F., and Team, S.S., 2009, Palynomorphs from a sediment core reveal a sudden remarkably warm Antarctica during the middle Miocene: Geology, v. 37, no. 10, p. 955–958, https://doi.org/10.1130/G30139A.1.

Wellner, J., Heroy, D., and Anderson, J., 2006, The death mask of the Antarctic ice sheet: Comparison of glacial geomorphic features across the continental shelf: Geomorphology, v. 75, no. 1-2, p. 157–171, https://doi.org/10.1016/j.geomorph.2005.05.015.

Wingfield, R., 1990, The origin of major incisions within the Pleistocene deposits of the North Sea: Marine Geology, v. 91, no. 1-2, p. 31–52, https://doi.org/10.1016/0025-3227(90)90131-3.

Wingham, D.J., Siegert, M.J., Shepherd, A., and Muir, A.S., 2006, Rapid discharge connects Antarctic subglacial lakes: Nature, v. 440, no. 7087, p. 1033–1036, https://doi.org/10.1038/nature04660.

Wright, A., Young, D., Roberts, J., Schroeder, D., Bamber, J., Dowdeswell, J., Young, N., Le Brocq, A., Warner, R., Payne, A., Blankenship, D.D., van Ommen, T.D., and Siegert, M.J., 2012, Evidence of a hydrological connection between the ice divide and ice sheet margin in the Aurora Subglacial Basin, East Antarctica: Journal of Geophysical Research–Earth Surface, v. 117, no. F1, F01033, https://doi.org/10.1029/2011JF002066.

Young, D.A., Wright, A.P., Roberts, J.L., Warner, R.C., Young, N.W., Greenbaum, J.S., Schroeder, D.M., Holt, J.W., Sugden, D.E., Blankenship, D.D., et al., 2011, A dynamic early East Antarctic Ice Sheet suggested by ice-covered fjord landscapes: Nature, v. 474, no. 7349, p. 72–75, https://doi.org/10.1038/nature10114.

Zachos, J., Pagani, M., Sloan, L., Thomas, E., and Billups, K., 2001a, Trends, rhythms, and aberrations in global climate 65 Ma to present: Science, v. 292, no. 5517, p. 686–693, https://doi.org/10.1126/science.1059412.

Zachos, J.C., Shackleton, N.J., Revenaugh, J.S., Pälike, H., and Flower, B.P., 2001b, Climate response to orbital forcing across the Oligocene-Miocene boundary: Science, v. 292, no. 5515, p. 274–278, https://doi.org/10.1126/science.1058288.

Zurbuchen, J.M., Gulick, S.P., Walton, M.A., and Goff, J.A., 2015, Imaging evidence for Hubbard Glacier advances and retreats since the Last Glacial Maximum in Yakutat and Disenchantment Bays, Alaska: Geochemistry Geophysics Geosystems, v. 16, no. 6, p. 1962–1974, https://doi.org/10.1002/2015GC005815.

Zwally, H.J., Giovinetto, M.B., Li, J., Cornejo, H.G., Beckley, M.A., Brenner, A.C., Saba, J.L., and Yi, D., 2005, Mass changes of the Greenland and Antarctic ice sheets and shelves and contributions to sea-level rise: 1992–2002: Journal of Glaciology, v. 51, no. 175, p. 509–527, https://doi.org/10.3189/172756505781829007.